Interleukin-17 regulates matrix metalloproteinase activity in human pulmonary tuberculosis

Shivani Singh[1], George Maniakis-Grivas[1], Utpal K Singh[2], Radha M Asher[1], Francesco Mauri[3], Paul T Elkington[1], Jon S Friedland[1*]

[1]Infectious Diseases and Immunity, Imperial College, Hammersmith Campus, Du Cane Road, London, UK;

[2]Tuberculosis Unit, Department of Medicine, Nalanda University Hospitals, Agam Kuan, Patna, India;

[3]Department of Histopathology, Hammersmith Hospitals, Imperial College London, UK.

Correspondence to: Jon S Friedland, Infectious Diseases and Immunity, Imperial College, Hammersmith Campus, Du Cane Road, London, SW12 0NN, UK.

Email: j.friedland@imperial.ac.uk

Conflict of interests statement

The authors hereby confirm that they do not have any conflicts of interest to declare.

Running Title: Interleukin-17 and MMPs in Human Tuberculosis

Word count: ~4158

Abstract

Tuberculosis (TB) is characterised by extensive pulmonary matrix breakdown. Interleukin-17 (IL-17) is key in host defence in TB but its role in TB-driven tissue damage is unknown. We investigated the hypothesis that respiratory stromal cell matrix metalloproteinase (MMP) production in TB is regulated by T helper-17 (T_H-17) cytokines. Biopsies of patients with pulmonary TB were analysed by immunohistochemistry (IHC) and patient bronchoalveolar lavage fluid (BALF) MMP and cytokine concentrations measured by Luminex assays. Primary human airway epithelial cells were stimulated with conditioned medium from human monocytes infected with *Mycobacterium tuberculosis* (Mtb) and T_H-17 cytokines. MMP secretion, activity and gene expression were determined by ELISA, Luminex assay, zymography, RT-qPCR and dual luciferase reporter assays. Signalling pathways were examined using phospho-western analysis and siRNA. IL-17 is expressed in TB patient granulomas and MMP-3 is expressed in adjacent pulmonary epithelial cells. IL-17 had a divergent, concentration-dependent effect on MMP secretion, increasing epithelial secretion of MMP-3 ($p<0.001$) over 72 h whilst decreasing that of MMP-9 ($p<0.0001$); mRNA levels were similarly affected. Both IL-17 and Interleukin-22 (IL-22) increased fibroblast Mtb-dependent MMP-3 secretion but IL-22 did not modulate epithelial MMP-3 expression. Both IL-17 and IL-22, but not Interleukin-23 (IL-23), were significantly upregulated in BALF from TB patients. IL-17-driven MMP-3 was dependent on p38 MAP kinase and the PI 3-K p110α subunit. In summary, IL-17 drives airway stromal cell-derived MMP-3, a mediator of tissue destruction in TB, both alone and via monocyte-dependent networks in TB. This is regulated by p38 MAP kinase and PI3-K pathways.

Key words: Mycobacteria, MMP, innate immunity, T_H-17, immunopathology.

Introduction

Mycobacterium tuberculosis (Mtb) has evolved adaptive mechanisms to evade host immunity with such success that today it is the number one infectious killer in the world and caused 1.3 million deaths in 2016 (www.who.int/tb/publications/global_report/en/). Cavities are pivotal to spread of TB but the mechanisms that drive them are less well understood [1]. Diverse studies indicate that host matrix metalloproteinases (MMPs) are key [2,3] and we recently showed that collagen destruction may be a key initial event triggering caseous necrosis [4]. MMPs can degrade all ECM components including type I collagen at neutral pH [5]. High MMP-9 concentrations correlated with disease severity and presence of granulomas in tuberculous pleurisy [6]. A matrix-degrading phenotype in human TB where MMP activity was relatively unopposed by specific Tissue Inhibitors of Matrix Metalloproteinases (TIMPs) was first described by our group [7]. MMP-1 and MMP-3 concentrations are increased in respiratory secretions of TB patients [8]. In the rabbit model, MMP-1 expression was greater in TB cavities and a MMP-1/TIMP imbalance was associated with development of cavities containing very high bacterial burdens [9]. A study in the zebrafish model showed that MMP-9 from epithelial cells, induced by the mycobacterial virulence factor ESAT-6, enhanced macrophage recruitment [10], thereby implicating MMPs in immunoregulatory as well as tissue destructive roles in TB.

Respiratory epithelial and other stromal cells are central in host defence to Mtb in addition to phagocytic cells such as alveolar macrophages. Respiratory epithelial cells secrete inflammatory mediators such as chemokines [11,12], interferon-γ (IFN-γ) and antimicrobial human β defensins [13]. MMP-1 and MMP-9 secretion from bronchial epithelial cells is up-regulated via TB-dependent cellular networks [14]. Another stromal cell, the lung fibroblast, also secretes mediators that limit the local growth of Mtb [15]. Such networks between leukocytes and stromal cells appear key both in host defence and in driving innate inflammatory tissue damage.

THelper-1 (T_H-1) cells have historically been thought to be necessary in control of Mtb infection but T_H-17 cells have now been identified as pivotal in Mtb control [16]. IL-17 is a pro-inflammatory cytokine that functions via mesenchymal and myeloid cells to induce secretion of diverse cytokines, chemokines, antimicrobial peptides and MMPs [17-19]. Mice with a genetically-inactivated IL-17 receptor were unable to exert long-term control of Mtb, despite a functional T_H-1 response [20]. IL-17 knockout mice failed to develop mature granulomas in Bacillus Calmette Guerin (BCG)-infected lung and had impaired protection from virulent Mtb [21]. Although IL-17 is dispensable for immunity against lab-adapted strains of Mtb, infection with the hypervirulent W-Beijing strain HN878 required IL-17 for early immunity [22]. In cynomolgus macaques, sterile granulomas had a higher frequency of T cells producing IL-17 [23] and pulmonary delivery of BCG vaccine triggered a mucosal immune response orchestrated by IL-17 [24]. Finally, in a study in the Chinese Han population, genetic polymorphisms in IL-17A and IL-17F were associated with host susceptibility to TB [25].

IL-22, a second T_H-17 family cytokine, has both anti- and pro-inflammatory activity at mucosal interfaces [26]. IL-22 produced by human NK cells inhibits the growth of Mtb by enhancing phagolysosomal fusion due to enhanced expression of calgranulin A [27]. IL-22 was also produced by human NK cells in TB pleural fluid in response to BCG and Mtb-related antigens, suggesting it might participate in the recall immune response for Mtb infection [28]. IL-17 and IL-22 function synergistically to induce epithelial mediators such as human β-defensin-2, S100 and lipocalin-2 [29]. IL-23, a member of the Interleukin-12 (IL-12) family, is essential for stabilisation and polarisation of lymphocytes towards a T_H-17 phenotype and promotes IL-17 secretion by activated T_H-17 cells [30]. *IL-23* mRNA was up-regulated in unfractionated BAL cells from TB patients compared to controls [31] and pulmonary IL-23 gene delivery with a

vaccine adjuvant augmented the expansion of Mtb-specific CD4+ T cells which produced IL-17 [32,33], with simultaneous reduction in mycobacterial burden and pulmonary inflammation.

Therefore, accumulating evidence suggests a central role for T_H-17 cytokines in host-pathogen interactions in TB. We hypothesized that in TB-dependent networks, stromal cell MMP secretion is regulated by T_H-17 cytokines. First, we identified IL-17 expression in lymphocytes around pulmonary granulomas in TB patients. Next, we showed that IL-17 increased mRNA expression and secretion of epithelial MMP-3, which was highly expressed in respiratory epithelial cells in TB patients. In contrast, IL-17 decreased respiratory epithelial cell MMP-9 production. Both IL-17 and IL-22 increased fibroblast MMP-3 secretion and we demonstrated for the first time that both these cytokines are elevated in BALF from TB patients. Finally, we investigated the mechanisms involved in IL-17 signalling and show that p38 mitogen activated protein kinase (MAPK) and the p110α subunit phosphoinositide 3-kinase (PI3K) signalling paths are key.

Materials and Methods

For further details, including experimental design and statistical methods please refer to supplementary material online files

Immunohistochemical analysis of patient biopsies

The project was approved by the Hammersmith and Queen Charlotte's & Chelsea Research Ethics Committee, London (Ref 07/H0707/120). Immunohistochemistry (IHC) was performed on paraffin embedded lung biopsies. Antibodies were purchased from Abcam, Cambridge, UK.

Clinical study

BALF samples were collected from patients being routinely investigated for respiratory symptoms at Nalanda University Hospitals, Patna, India. The study was approved by the ethics review board at Nalanda Medical College and University Hospitals (Reference Number SS/0810/TB). Samples were centrifuged and sterile filtered to remove cellular debris and Mtb [34].

Monocyte purification, infection and generation of CoMTb

Primary blood mononuclear cells (PBMCs) were from two donor buffy coats from healthy donors (National Blood Transfusion Service, UK). Monocytes were infected with Mtb H37Rv strain at a multiplicity of infection of 1. For epithelial cells, Ziehl-Nielsen staining demonstrated that 30% cells were infected at a MOI of 10, which is similar to previous reports [35]. Medium from infected monocytes was termed conditioned medium from monocytes infected with Mtb (CoMTb). Control medium was generated in an identical manner but without infection and was called CoMCont.

Cell culture and experimental design

Primary small airway epithelial cells (SAEC) and normal human bronchial epithelial cells (NHBE) were cultured in bronchial epithelial growth media (Lonza Biosciences, Basel, Switzerland) and human MRC-5 fibroblasts were grown in Eagle's medium (Sigma-Aldrich, Gillingham, Dorset, UK), as per suppliers' instructions. Epithelial cells were stimulated with a 1 in 5 dilution of CoMTb and MRC-5 cells with a 1 in 50 dilution. Supernatants were harvested at 72h for secretion analysis and mRNA extraction was performed at 24h [14,36].

Promoter-reporter assay

Promoter-reporter studies were performed using FuGENE HD Transfection Reagent and Promega's Dual-Luciferase Reporter Assay System (Promega-UK, Southampton, Hampshire, UK). The MMP-3 promoter (1206 base pairs) was linked to firefly luciferase and the reference gene thymidine kinase promoter was linked to *Renilla* luciferase.

Phospho-western analysis and gelatin zymography

After electrophoresis, proteins were electro-transferred to nitrocellulose membranes and probed with a primary antibody, then washed and incubated with a secondary antibody. Luminescence was produced using the ECL system. MMP-9 gelatinolytic activity was detected by zymography using standard methodology [37].

Small interfering (siRNA) transfection

All siRNAs pools targeted the transcription products from 4 alleles of the gene of interest. Conditions for transfection were optimised using a transfection control and a negative control (non-targeting siRNA, supplementary material, Figure S1).

RNA extraction, cDNA synthesis and reverse transcription- quantitative polymerase chain reaction (RT-qPCR)

RNA extraction was performed using the Qiagen RNeasy Minikit (QIAGEN Ltd, Manchester, UK). cDNA synthesis was performed using a Qiagen Quantitect reverse transcription kit (QIAGEN Ltd, Manchester, UK). Real-time quantitative PCR was performed using the Brilliant II QPCR master mix on the Stratagene Mx3000P platform (Stratagene, Cambridge, UK). MMP primers and probes have been described previously [38]. Experimental MMP data was normalized to three reference genes. Analysis of MMP mRNA expression was first undertaken

by the standard curve method, and results corroborated by C_T values assessing levels of gene expression.

Results

IL-17 is expressed in human TB granulomas and has divergent effects on epithelial cell MMP-3 and MMP-9 secretion

First, we investigated the expression of IL-17 in 5 TB and 5 control human lung biopsy specimens. IL-17 was expressed TB granulomas (Figure 1A) but not in control lung biopsies of normal tissue (Figure 1B). As a positive control, we detected colonic T lymphocyte immunoreactivity (Supplementary material, Figure S2A). No staining was seen when the primary antibody was omitted as a negative control (Supplementary material, Figure S2B). Next, we investigated MMP secretion from human distal small airway epithelial cells (SAECs). MMP-1, MMP-3 and MMP-9 secretion from SAECs were all increased following stimulation by CoMTb at a 1 in 5 dilution. MMP-3 secretion increased 2.2-fold from 534±34 pg/ml to 1171±44 pg/ml (Figure 1C, p=0.005) and MMP-9 secretion, 10.5-fold from 11446±15 pg/ml to 119561±77 pg/ml (Figure 1D, p=0.002). MMP-1 secretion increased 4.5-fold from a baseline of 490±30 pg/ml to 2247±25 pg/ml (Figure 1E, p=0.008). SAECs constitutively secrete MMP-2 at a baseline which was not altered significantly by CoMTb (Figure 1F). MMP-8 was detectable but only at very low concentrations (Figure 1G). MMP-7, -12 and -13 were almost undetectable (data not shown).

Next, we investigated the effect of IL-17 on MMP secretion. In SAECs, maximal MMP-3 secretory effect was observed with 30 ng/ml IL-17 (Supplementary material, Figure S3A)

[39,40]. In co-stimulation experiments with CoMtb, IL-17 increased baseline epithelial MMP-3 secretion from 534±34 pg/ml to 1612±17 pg/ml ($p<0.001$) and CoMTb-driven MMP-3 secretion from 1171±44 pg/ml to 4196±28 pg/ml (Figure 1C, $p<0.001$). In contrast, CoMTb-driven MMP-9 secretion was suppressed by IL-17 from 119561±77 pg/ml to 7483±50 pg/ml (Figure 1D, $p<0.0001$). MMP-9-induced gelatinolysis, measured by zymography, was similarly decreased by IL-17 (data not shown). Changes in gene expression were consistent with secretion data (data not shown). IL-17 did not alter MMP-1, MMP-2 or MMP-8 secretion from SAECs (Figure 1E-G). Lastly, we investigated TIMP-1/2 secretion as the MMP/ TIMP ratio is functionally important in determining net matrix degradation. CoMTb suppressed TIMP-1 secretion (Supplementary material, Figure S3B, $p<0.5$) but IL-17 did not significantly modulate this. TIMP-2 secretion was also unaffected by IL-17 (Supplementary material, Figure S3C), therefore these results confirm that up-regulation of MMP-3 in TB is unopposed by inhibitor secretion.

MMP-3 is expressed by epithelial cells in TB and secretion is up-regulated by IL-17 in a TB network, whereas direct infection with Mtb does not modulate expression

In TB patient lung biopsies, pulmonary epithelial cells adjacent to TB granulomas strongly expressed MMP-3 (Figure 2A), whereas minimal staining was observed in normal lung biopsies (Figure 2B). After confirming that upper airway epithelial cells (NHBE) and SAECs had similar secretion profiles, we performed all further experiments on NHBE cells. Our immunohistochemical studies showed MMP-3 expression by epithelial cells in the relatively larger airways, which we felt were best modelled by NHBEs, and hence we used these for further studies. In NHBEs, maximal MMP-3 secretory effect was observed with 10 ng/ml of IL-17 (Supplementary material, Figure S3D) [41,42]. Kinetic experiments in NHBE cells showed that MMP-3 concentrations peaked at 72 h when stimulated with IL-17, after which it declined (Figure 2C, $p<0.001$) and IL-17 driven MMP-3 mRNA accumulation peaked at 24 h (Figure 2D,

p<0.01). These kinetics are similar to our published data on MMP-1 and -9 secretion [14,36]. Next, we investigated the regulation of MMP-3 and MMP-9 by IL-22 and IL-23 and found no change (Supplementary material, Figure S4, A-D). Direct infection with Mtb at multiplicity of infection from 0.1-10 had no significant effect on MMP-3 secretion from NHBE cells in the presence or absence of IL-17 (Figure 2E). Infection at a higher MOI did not increase uptake of bacteria and MMP production remained unchanged (data not shown).

To further dissect the IL-17 and CoMTb-driven MMP-3 up-regulation, we performed cytokine and chemokine analyses in the supernatants from NHBEs stimulated with IL-17 alone or in combination with CoMTb. The cytokines and chemokines analysed were IL-1β, IL-6, IL-10, TNF-α, IL-1Ra, IFN-α, IFN-γ, IL-13, IL-15, IL-17, IL-12, IL-5, IL-2, IL-7, IL-2R, IL-4, RANTES, Eotaxin, MIP-1β, MIP-1α, MCP-1, IP-10, MIG and CXCL-8. We found that although TNF-α, IL-1RA, CXCL-8 and MIP-1α were elevated in both groups, only CXCL-8 concentration was significantly different between groups (Supplementary material, Table S1, p<0.001). Stimulating NHBE cells with TNF-α alone and in the presence of IL-17 did not drive MMP-3 secretion (Supplementary material, Figure S5). These experiments demonstrate that synergy between multiple mediators drives maximal MMP-3 production from stromal cells in TB.

IL-17 and IL-22 augment TB-dependent MMP-3 secretion from fibroblasts

Next, we investigated MMP secretion from fibroblasts, stromal cells that can secrete high concentrations of MMPs [43]. CoMTb stimulation drove a concentration-dependent increase in MMP-3 secretion from MRC-5 fibroblasts at 72 h (Fig 3A). Although maximal MMP-3 secretion was observed at a CoMTb dilution of 1 in 5 (p<0.0001), this was accompanied with

significant cell death. In subsequent experiments, CoMTb was used at a dilution of 1 in 50, which also significantly up-regulated MMP-3 secretion ($p<0.01$) with no effect on cell viability. To investigate further, promoter-reporter studies were performed using a wild-type construct of the MMP-3 promoter. Activation in response to CoMTb was detectable at 6 h, peaking at 24 h, and thereafter remaining stable for 48 h (Figure 3B, $p<0.001$).

Next, MRC-5 fibroblasts were stimulated with IL-17 alone and in combination with CoMTb. IL-17 further up-regulated CoMTb-induced MMP-3 secretion from 107005 ±6729 pg/ml to 191829 ±11057 pg/ml (Figure 3C, $p<0.001$), but did not affect MMP-3 as a single stimulus. Similarly, IL-22 almost doubled fibroblast MMP-3 secretion from 16694 ±1734 pg/ml to 27638 ±483 pg/ml (Figure 3D, $p<0.001$), but did not affect baseline MMP-3 secretion in the absence of CoMTb.

IL-17 and IL-22 are up-regulated in TB patient bronchoalveolar lavage fluid

To examine the relevance of these findings to human TB infection, we investigated IL-17, IL-22 and IL-23 concentrations in BALF from 17 well-characterized patients with confirmed pulmonary TB and 18 well-matched respiratory symptomatic patients with other diagnoses that may cause a clinically similar picture, which we have previously been reported [44]. There were no significant differences between the two groups with regards to age, gender, and smoking history. None of the subjects had a previous history of TB. The median IL-17 concentration was increased in TB patients compared to other respiratory symptomatic patients ($p=0.02$) although the absolute concentrations detectable in BALF were low (Fig 4A). The median IL-22 concentration in BALF from TB patients was 4-fold higher than in control patients (Figure 4B, $p=0.006$). IL-23 concentrations were virtually all below the level of detection in both control and TB groups (Supplementary material, Figure S6). This demonstrates that the IL-17

expression seen in lymphocytes by IHC leads to increased concentrations in bronchial lining fluid.

IL-17 driven MMP-3 secretion is p38 MAPK dependent

Next, we investigated the mechanisms regulating IL-17-dependent MMP-3 secretion from NHBE cells. First, we studied the MAPK pathways. Both CoMTb and IL-17 as single stimuli caused phosphorylation of p38 MAPK peaking at 30 min after which it returned to baseline. Phosphorylation of p38 was further increased when cells were co-stimulated with 10ng/ml of IL-17 and CoMTb (Figure 5A). Densitometric analysis confirmed increased phosphorylation. ERK 1/2 and JNK MAPKs are constitutively phosphorylated in NHBE cells and were not investigated further.

Next, we investigated the effect of chemical and siRNA mediated inhibition of p38 on IL-17-dependent MMP-3 secretion. The p38 specific chemical inhibitor SB203580 suppressed IL-17 driven MMP-3 secretion in a concentration-dependent manner to baseline (Figure 5B, $p<0.001$). Concurrently, inhibition of IL-17-dependent MMP-3 mRNA accumulation was also observed (Figure 5C, $p<0.001$). Confirming these data, p38 MAPK specific siRNA decreased IL-17/CoMTb driven MMP-3 secretion by 50% (Figure 5D, $p<0.01$) and mRNA expression to baseline levels (Figure 5E, $p<0.01$). The suppression was maximal with 30 nM of the siRNA. Cells were also transfected with non-targeting siRNA (NT siRNA) and no change was observed. siRNA knockdown of phospho-p38 was confirmed by western blotting and at the mRNA level (Supplementary material, Figure S7A and B). Significant knockdown was observed at 10nM of p38 siRNA and levels were undetectable with 30nM of siRNA in NHBEs stimulated with CoMTb and 10ng/ml of IL-17. Non-targeting siRNA had no effect on p38 expression. Similar results with p38 chemical and siRNA mediated inhibition were observed in SAECs (data not

shown). In summary, these data show that the p38 MAPK signalling regulates IL-17-driven MMP-3 secretion from NHBE cells in a TB network.

Epithelial MMP-3 secretion in TB is regulated by the PI3K p110α subunit and AKT

Finally, we investigated whether the PI3Kinase pathway had a role in IL-17 driven MMP-3 up-regulation, since this path has been implicated in the IL-17A mediated regulation of several other genes in human airway epithelial cells [39]. The non-specific PI3Kinase proximal catalytic subunit inhibitor LY294002 suppressed IL-17-dependent MMP-3 secretion to control concentrations (Figure 6A, $p<0.0001$). To identify the specific p110 catalytic subunit involved, NHBE's were transfected with siRNAs specific for the p110 catalytic subunit isoforms. MMP-3 mRNA was suppressed to baseline with the p110α-specific inhibitor (Figure 6B, $p<0.0001$). There was no change upon pre-incubation with non-targeting siRNA, the negative control. In contrast, p110β subunit specific inhibition did not alter MMP production (data not shown). siRNA knockdown of p110α subunit was confirmed by western blotting and at the mRNA level (Supplementary material, Figure S7C and D). Significant knockdown was observed at 10nM and levels were undetectable with 30nM of siRNA, with no effect seen with non-targeting siRNA.

As the γ and δ isoforms are almost exclusively expressed in leukocytes, they were not investigated. Downstream of PI3Kinase, inhibition of AKT similarly suppressed MMP-3 secretion to baseline (Figure 6C, $p<0.0001$). Thus both proximal and distal nodes of the PI3Kinase signalling pathway regulate IL-17 mediated MMP-3 gene expression and secretion in TB.

Discussion

We demonstrate for the first time that IL-17 is expressed within human TB granulomas and adjacent epithelial cells express MMP-3. IL-17 causes up-regulation of MMP-3 gene expression and secretion from epithelial cells exposed to a monocyte-dependent infection *in-vitro* network. Since SAECs and NHBEs have different immunological roles [45], we first investigated their secretion profiles and identified this to be similar. IHC showed epithelial MMP-3 expression in the relatively larger airways, which we felt were best modelled by NHBEs, and hence we used them for further studies. We have previously shown that MRC-5 fibroblasts and human lung (HL) fibroblasts have similar MMP production profiles in a TB network [43] and therefore we chose to focus on one fibroblast cell line for this study. Both T_H-17 cytokines, IL-17 and IL-22, drive MMP-3 secretion from MRC-5 fibroblasts exposed to CoMTb. In contrast, IL-17 did not modulate the effects of direct infection by Mtb. Concentrations of both these cytokines were elevated in BALF from pulmonary TB patients but not from other patients with similar respiratory symptoms. We have defined key mechanisms through which IL-17 regulates MMP-3, which is a mediator of tissue damage in TB, in part through its action activating the collagenase MMP-1 [46]. Together these data define a new role for IL-17 in up-regulating tissue-destructive proteases in TB, in addition to previously described functions in granuloma development and control of infection [20,21].

The action of IL-17 to increase baseline and CoMTb-driven epithelial cell MMP-3 gene expression and secretion is consistent with other studies. In murine embryonic fibroblasts, IL-17 regulated chemokine and MMP (MMPs-3, -9 and -13) expression to recruit both neutrophils and monocytes [47]. IL-17 and MMP-3 were expressed in TB lymphocytes and lung epithelial cells, but IL-17 did not drive epithelial MMP-3 when cells were directly infected with Mtb. A biologically relevant feature of IL-17 is its strong cooperative and synergistic effect via mRNA

stabilisation of other inflammatory cytokines [48], which may account for its effect on MMP-3 secretion in the TB network between epithelial cells and monocytes. In contrast, CoMTb-driven MMP-9 secretion and gene expression were suppressed by IL-17 and functional activity of MMP-9 was also reduced. Oriss, et al [49] recently showed that IL-23-dependent IL-17 gene expression in lung dendritic cells is negatively regulated by MMP-9 enzymatic activity, suggesting that inhibition of MMP-9 could facilitate a strong T_H-17 response which is desirable for vaccination against Mtb.

To further dissect the IL-17 and CoMTb-driven MMP-3 up-regulation, we performed an extensive cytokine and chemokine analyses in the supernatants from stimulated NHBEs and found that only CXCL-8 concentration was significantly higher in the TB/ IL-17 network. Stimulating NHBE cells with TNF-α alone and in the presence of IL-17 did not drive MMP-3 secretion. TNF-α concentration in CoMTb is 157 pg/ml when used at a 1 in 5 dilution (supplementary material, Table S2). When NHBE's were stimulated with 5ng/ml of TNF-α (30-fold more), this was a weak stimulus to MMP-9 secretion, alone and in combination with lipoarabinomannan (LAM) [14]. Similarly, TNF-α alone was a weak stimulus to MMP-1 secretion from epithelial cells [36]. In a previous study investigating direct infection of human macrophages with Mtb, other stimuli such as LPS, BCG and individual cytokines including TNF-α, IL-1β or IFN-γ did not drive MMP-1 production [50]. Thus, synergy between different mediators appears key in Mtb-driven MMP production from stromal cells.

We also demonstrated that MMP-3 secretion and promoter activity was increased in fibroblasts as a result of a monocyte-dependent network in TB and that this effect was increased synergistically by both IL-22 and IL-17. This is consistent with data in rheumatoid arthritis where T_H-17 cells induced MMP-1 and -3 production [51]. In human cardiac fibroblasts, IL-17

stimulated MMP-1 expression via p38 and ERK dependent AP-1, NF-κB and C/EBP-β activation [52]. In the lung, fibroblasts can secrete very high MMP-1 concentrations [43]. IL-22 did not drive MMP secretion in epithelial cells (Supplementary material, Figure S3) which may reflect the divergent signalling paths activated in epithelial cells compared to fibroblasts. Unlike IL-17, IL-22 signals mainly via the Stat3 pathway and has a clonogenic and protective effect on human airway epithelial cells [53].

Next, we investigated whether the T_H-17 cytokines were elevated in BALF from patients with pulmonary TB. In a study of 20 pulmonary TB patients and 20 matched controls, plasma IL-17 levels were elevated in patients. IL-17 levels substantially decreased after treatment and correlated with both CRP and ESR [54]. Previous studies showed that IL-22 may be detected in tuberculous BALF, pleural fluid and pericardial fluid [55,56]. We confirmed that IL-22 was significantly up-regulated in BALF from TB patients and identified for the first time that IL-17 concentrations were also elevated in TB patients, although concentrations were low (Figure 4). It has been proposed that low levels of soluble IL-17 in TB is a result of inhibition of T_H-17 effectors by the T_H-1 effectors at the site of disease [57]. However, IL-17 levels in BALF and pleural fluid, even in the absence of such an inhibitory T_H-1 response, is frequently low or undetectable [56,58] and IL-17 cell-mediated inflammation is independent of IL-22 [59]. In contrast, IL-17 mRNA expression in pleural fluid mononuclear cells was increased by the Mtb peptides ESAT-6 and culture filtrate protein (CFP)-10 [57]. *In situ* hybridisation could be used as a further method to confirm increased IL-17 expression in lungs of TB patients.

Finally, we dissected key pathways regulating IL-17-dependent MMP-3 secretion. We demonstrated for the first time that inhibition of p38 MAPK, the PI3K p110α subunit and AKT resulted in abrogation of IL-17 driven MMP-3 up-regulation in a TB network. This finding is consistent with studies which showed that IL-17 regulates mucosal neutrophil immunity via

chemokines and growth factors [40]. It has been shown in human airway epithelial cells that IL-17 mediated induction of IL-19, CXCL-1, -2, -3, -5, and -6 human defence genes was mediated via the PI3K pathway [39]. In airway epithelial cells, regulation of MMPs in Mtb-dependent respiratory networks was identified to be via the distal rapamycin-sensitive PI 3-K/ $p70^{S6K}$ cascade, with the proximal p110α subunit augmenting MMP production [60]. IL-17 may enhance migration of periodontal ligament fibroblasts by increasing MMP-1 expression through p38 MAPK and NFκB signal transduction pathways [61]. IL-17 has been shown to limit Mtb-driven HIF-1α expression [62], showing that there is a complex interplay between inflammatory signalling, hypoxia and tissue destruction [63].

In summary, we investigated the effect of T_H-17 cytokines on epithelial MMP production by immunohistochemical analysis of patient biopsies, by investigating a cellular TB network model and finally by cytokine analysis of BALF from TB patients. We specifically focused on intercellular networks between lymphocytes and airway epithelial cells in TB and have shown for the first time that lymphocyte-derived IL-17 drives both epithelial- and fibroblast-derived MMP-3 in a TB network, whereas direct infection does not. IL-17 was expressed in the lymphocytes associated with TB granulomas and MMP-3 was expressed in the epithelial cells around these TB granulomas. MMP-3 expression was regulated by the p38 MAP Kinase path and the proximal (p110α subunit) and distal nodes (AKT) of the PI3K pathway. The effects are MMP-specific as MMP-9 secretion was down-regulated. On examination of BALF from patients with TB, IL-17 and IL-22 were both detectable. Several biologics such as monoclonal antibodies that neutralize IL-17 signalling are now in clinical development [64,65]. In the context of TB modulating the T_H-17 pathway may alter MMP activity, reduce tissue destruction and improve outcomes. In the present era of increasing antimycobacterial drug resistance, host directed therapy is emerging as a key paradigm for future TB treatment [66].

Funding Information

Shivani Singh was funded by a Medical Research Council (UK) Training Fellowship. JSF and PE acknowledge support of the Imperial College NIHR Biomedical Research Centre.

Acknowledgements

We thank Dr. Rajniti Singh, Mr. Ramji Prasad, Mr Balram Singh, Dr. Ajay Singh and Dr. Sandeep Sen for help with the clinical study in India. We are grateful to Dr Ashley Whittington at Imperial College London for his overall help with the project. We would also like to thank Alex Bowman, Histopathology Core Facility Laboratory Manager at the Respiratory Research Centre, Royal Brompton Hospital and Steve Rothery at FILM, Imperial College London for their help with immunohistochemistry.

Author contributions statement

SS designed and performed experiments, analysed data and prepared first draft of manuscript. GMG performed experiments on MRC-5 fibroblasts. UKS designed and conducted the clinical study. FM performed the immunohistochemical analyses. PTE was involved in experimental design, analysis and interpretation of data as well as preparation of final manuscript. JSF was the Principal Investigator who conceived the project and was responsible for overall direction of the study, interpretation of data and writing of the final manuscript.

References

1. Chang KC, Yew WW, Tam CM*, et al.* WHO group 5 drugs and difficult multidrug-resistant tuberculosis: a systematic review with cohort analysis and meta-analysis. *Antimicrob Agents Chemother* 2013; **57**: 4097-4104.
2. Elkington PT, D'Armiento JM, Friedland JS. Tuberculosis immunopathology: the neglected role of extracellular matrix destruction. *Sci Transl Med* 2011; **3**: 71ps76.
3. Ong CW, Elkington PT, Friedland JS. Tuberculosis, pulmonary cavitation, and matrix metalloproteinases. *Am J Respir Crit Care Med* 2014; **190**: 9-18.

4. Al Shammari B, Shiomi T, Tezera L*, et al.* The Extracellular Matrix Regulates Granuloma Necrosis in Tuberculosis. *The Journal of infectious diseases* 2015; **212**: 463-473.
5. Brinckerhoff CE, Matrisian LM. Matrix metalloproteinases: a tail of a frog that became a prince. *Nat Rev Mol Cell Biol* 2002; **3**: 207-214.
6. Hrabec E, Strek M, Zieba M*, et al.* Circulation level of matrix metalloproteinase-9 is correlated with disease severity in tuberculosis patients. *Int J Tuberc Lung Dis* 2002; **6**: 713-719.
7. Price NM, Farrar J, Tran TT*, et al.* Identification of a matrix-degrading phenotype in human tuberculosis in vitro and in vivo. *J Immunol* 2001; **166**: 4223-4230.
8. Elkington P, Shiomi T, Breen R*, et al.* MMP-1 drives immunopathology in human tuberculosis and transgenic mice. *J Clin Invest* 2011; **121**: 1827-1833.
9. Kubler A, Luna B, Larsson C*, et al.* Mycobacterium tuberculosis dysregulates MMP/TIMP balance to drive rapid cavitation and unrestrained bacterial proliferation. *J Pathol* 2015; **235**: 431-444.
10. Volkman HE, Pozos TC, Zheng J*, et al.* Tuberculous granuloma induction via interaction of a bacterial secreted protein with host epithelium. *Science* 2010; **327**: 466-469.
11. Wickremasinghe MI, Thomas LH, Friedland JS. Pulmonary epithelial cells are a source of IL-8 in the response to Mycobacterium tuberculosis: essential role of IL-1 from infected monocytes in a NF-kappa B-dependent network. *J Immunol* 1999; **163**: 3936-3947.
12. Sauty A, Dziejman M, Taha RA*, et al.* The T cell-specific CXC chemokines IP-10, Mig, and I-TAC are expressed by activated human bronchial epithelial cells. *J Immunol* 1999; **162**: 3549-3558.
13. Rivas-Santiago B, Contreras JC, Sada E*, et al.* The potential role of lung epithelial cells and beta-defensins in experimental latent tuberculosis. *Scand J Immunol* 2008; **67**: 448-452.
14. Elkington PT, Green JA, Emerson JE*, et al.* Synergistic up-regulation of epithelial cell matrix metalloproteinase-9 secretion in tuberculosis. *Am J Respir Cell Mol Biol* 2007; **37**: 431-437.
15. O'Kane CM, Boyle JJ, Horncastle DE*, et al.* Monocyte-dependent fibroblast CXCL8 secretion occurs in tuberculosis and limits survival of mycobacteria within macrophages. *Journal of immunology (Baltimore, Md : 1950)* 2007; **178**: 3767-3776.
16. Torrado E, Cooper AM. IL-17 and Th17 cells in tuberculosis. *Cytokine Growth Factor Rev* 2010; **21**: 455-462.
17. Trajkovic V, Stosic-Grujicic S, Samardzic T*, et al.* Interleukin-17 stimulates inducible nitric oxide synthase activation in rodent astrocytes. *J Neuroimmunol* 2001; **119**: 183-191.
18. Fossiez F, Djossou O, Chomarat P*, et al.* T cell interleukin-17 induces stromal cells to produce proinflammatory and hematopoietic cytokines. *J Exp Med* 1996; **183**: 2593-2603.
19. Jovanovic DV, Di Battista JA, Martel-Pelletier J*, et al.* IL-17 stimulates the production and expression of proinflammatory cytokines, IL-beta and TNF-alpha, by human macrophages. *J Immunol* 1998; **160**: 3513-3521.
20. Freches D, Korf H, Denis O*, et al.* Mice genetically inactivated in interleukin-17A receptor are defective in long-term control of Mycobacterium tuberculosis infection. *Immunology* 2013; **140**: 220-231.
21. Okamoto Yoshida Y, Umemura M, Yahagi A*, et al.* Essential role of IL-17A in the formation of a mycobacterial infection-induced granuloma in the lung. *J Immunol* 2010; **184**: 4414-4422.
22. Gopal R, Monin L, Slight S*, et al.* Unexpected role for IL-17 in protective immunity against hypervirulent Mycobacterium tuberculosis HN878 infection. *PLoS Pathog* 2014; **10**: e1004099.
23. Gideon HP, Phuah J, Myers AJ*, et al.* Variability in Tuberculosis Granuloma T Cell Responses Exists, but a Balance of Pro- and Anti-inflammatory Cytokines Is Associated with Sterilization. *PLoS Pathog* 2015; **11**: e1004603.
24. Aguilo N, Alvarez-Arguedas S, Uranga S*, et al.* Pulmonary but Not Subcutaneous Delivery of BCG Vaccine Confers Protection to Tuberculosis-Susceptible Mice by an Interleukin 17-Dependent Mechanism. *The Journal of infectious diseases* 2016; **213**: 831-839.
25. Wang M, Xu G, Lu L*, et al.* Genetic polymorphisms of IL-17A, IL-17F, TLR4 and miR-146a in association with the risk of pulmonary tuberculosis. *Sci Rep* 2016; **6**: 28586.

26. Sonnenberg GF, Fouser LA, Artis D. Border patrol: regulation of immunity, inflammation and tissue homeostasis at barrier surfaces by IL-22. *Nat Immunol* 2011; **12**: 383-390.
27. Dhiman R, Venkatasubramanian S, Paidipally P*, et al.* Interleukin 22 inhibits intracellular growth of Mycobacterium tuberculosis by enhancing calgranulin A expression. *J Infect Dis* 2014; **209**: 578-587.
28. Fu X, Yu S, Yang B*, et al.* Memory-Like Antigen-Specific Human NK Cells from TB Pleural Fluids Produced IL-22 in Response to IL-15 or Mycobacterium tuberculosis Antigens. *PLoS One* 2016; **11**: e0151721.
29. McAleer JP, Kolls JK. Directing traffic: IL-17 and IL-22 coordinate pulmonary immune defense. *Immunol Rev* 2014; **260**: 129-144.
30. Aggarwal S, Ghilardi N, Xie MH*, et al.* Interleukin-23 promotes a distinct CD4 T cell activation state characterized by the production of interleukin-17. *J Biol Chem* 2003; **278**: 1910-1914.
31. Dheda K, Chang JS, Lala S*, et al.* Gene expression of IL17 and IL23 in the lungs of patients with active tuberculosis. *Thorax* 2008; **63**: 566-568.
32. Wozniak TM, Ryan AA, Britton WJ. Interleukin-23 restores immunity to Mycobacterium tuberculosis infection in IL-12p40-deficient mice and is not required for the development of IL-17-secreting T cell responses. *J Immunol* 2006; **177**: 8684-8692.
33. Happel KI, Lockhart EA, Mason CM*, et al.* Pulmonary interleukin-23 gene delivery increases local T-cell immunity and controls growth of Mycobacterium tuberculosis in the lungs. *Infect Immun* 2005; **73**: 5782-5788.
34. Elkington PT, Green JA, Friedland JS. Filter sterilization of highly infectious samples to prevent false negative analysis of matrix metalloproteinase activity. *Journal of immunological methods* 2006; **309**: 115-119.
35. Bermudez LE, Goodman J. Mycobacterium tuberculosis invades and replicates within type II alveolar cells. *Infection and immunity* 1996; **64**: 1400-1406.
36. Elkington PT, Emerson JE, Lopez-Pascua LD*, et al.* Mycobacterium tuberculosis up-regulates matrix metalloproteinase-1 secretion from human airway epithelial cells via a p38 MAPK switch. *J Immunol* 2005; **175**: 5333-5340.
37. Leber TM, Balkwill FR. Zymography: a single-step staining method for quantitation of proteolytic activity on substrate gels. *Analytical biochemistry* 1997; **249**: 24-28.
38. Nuttall RK, Pennington CJ, Taplin J*, et al.* Elevated membrane-type matrix metalloproteinases in gliomas revealed by profiling proteases and inhibitors in human cancer cells. *Molecular cancer research : MCR* 2003; **1**: 333-345.
39. Huang F, Kao CY, Wachi S*, et al.* Requirement for both JAK-mediated PI3K signaling and ACT1/TRAF6/TAK1-dependent NF-kappaB activation by IL-17A in enhancing cytokine expression in human airway epithelial cells. *J Immunol* 2007; **179**: 6504-6513.
40. McAllister F, Henry A, Kreindler JL*, et al.* Role of IL-17A, IL-17F, and the IL-17 receptor in regulating growth-related oncogene-alpha and granulocyte colony-stimulating factor in bronchial epithelium: implications for airway inflammation in cystic fibrosis. *J Immunol* 2005; **175**: 404-412.
41. Wong CK, Cao J, Yin YB*, et al.* Interleukin-17A activation on bronchial epithelium and basophils: a novel inflammatory mechanism. *Eur Respir J* 2010; **35**: 883-893.
42. Zijlstra GJ, Ten Hacken NH, Hoffmann RF*, et al.* Interleukin-17A induces glucocorticoid insensitivity in human bronchial epithelial cells. *Eur Respir J* 2012; **39**: 439-445.
43. O'Kane CM, Elkington PT, Jones MD*, et al.* STAT3, p38 MAPK, and NF-kappaB drive unopposed monocyte-dependent fibroblast MMP-1 secretion in tuberculosis. *American journal of respiratory cell and molecular biology* 2010; **43**: 465-474.
44. Singh S, Kubler A, Singh UK*, et al.* Antimycobacterial drugs modulate immunopathogenic matrix metalloproteinases in a cellular model of pulmonary tuberculosis. *Antimicrob Agents Chemother* 2014; **58**: 4657-4665.

45. Wickremasinghe MI, Thomas LH, O'Kane CM*, et al.* Transcriptional mechanisms regulating alveolar epithelial cell-specific CCL5 secretion in pulmonary tuberculosis. *The Journal of biological chemistry* 2004; **279**: 27199-27210.
46. Treadwell BV, Towle CA, Ishizue K*, et al.* Stimulation of the synthesis of collagenase activator protein in cartilage by a factor present in synovial-conditioned medium. *Arch Biochem Biophys* 1986; **251**: 724-731.
47. Qiu Z, Dillen C, Hu J*, et al.* Interleukin-17 regulates chemokine and gelatinase B expression in fibroblasts to recruit both neutrophils and monocytes. *Immunobiology* 2009; **214**: 835-842.
48. Ruddy MJ, Wong GC, Liu XK*, et al.* Functional cooperation between interleukin-17 and tumor necrosis factor-alpha is mediated by CCAAT/enhancer-binding protein family members. *J Biol Chem* 2004; **279**: 2559-2567.
49. Oriss TB, Krishnamoorthy N, Raundhal M*, et al.* Cutting Edge: MMP-9 inhibits IL-23p19 expression in dendritic cells by targeting membrane stem cell factor affecting lung IL-17 response. *J Immunol* 2014; **192**: 5471-5475.
50. Elkington PT, Nuttall RK, Boyle JJ*, et al.* Mycobacterium tuberculosis, but not vaccine BCG, specifically upregulates matrix metalloproteinase-1. *Am J Respir Crit Care Med* 2005; **172**: 1596-1604.
51. van Hamburg JP, Asmawidjaja PS, Davelaar N*, et al.* Th17 cells, but not Th1 cells, from patients with early rheumatoid arthritis are potent inducers of matrix metalloproteinases and proinflammatory cytokines upon synovial fibroblast interaction, including autocrine interleukin-17A production. *Arthritis Rheum* 2011; **63**: 73-83.
52. Cortez DM, Feldman MD, Mummidi S*, et al.* IL-17 stimulates MMP-1 expression in primary human cardiac fibroblasts via p38 MAPK- and ERK1/2-dependent C/EBP-beta , NF-kappaB, and AP-1 activation. *Am J Physiol Heart Circ Physiol* 2007; **293**: H3356-3365.
53. Aujla SJ, Chan YR, Zheng M*, et al.* IL-22 mediates mucosal host defense against Gram-negative bacterial pneumonia. *Nat Med* 2008; **14**: 275-281.
54. Xu L, Cui G, Jia H*, et al.* Decreased IL-17 during treatment of sputum smear-positive pulmonary tuberculosis due to increased regulatory T cells and IL-10. *J Transl Med* 2016; **14**: 179.
55. Matthews K, Wilkinson KA, Kalsdorf B*, et al.* Predominance of interleukin-22 over interleukin-17 at the site of disease in human tuberculosis. *Tuberculosis (Edinb)* 2011; **91**: 587-593.
56. Scriba TJ, Kalsdorf B, Abrahams DA*, et al.* Distinct, specific IL-17- and IL-22-producing CD4+ T cell subsets contribute to the human anti-mycobacterial immune response. *J Immunol* 2008; **180**: 1962-1970.
57. Qiao D, Yang BY, Li L*, et al.* ESAT-6- and CFP-10-specific Th1, Th22 and Th17 cells in tuberculous pleurisy may contribute to the local immune response against Mycobacterium tuberculosis infection. *Scand J Immunol* 2011; **73**: 330-337.
58. Molet S, Hamid Q, Davoine F*, et al.* IL-17 is increased in asthmatic airways and induces human bronchial fibroblasts to produce cytokines. *J Allergy Clin Immunol* 2001; **108**: 430-438.
59. van Hamburg JP, Corneth OB, Paulissen SM*, et al.* IL-17/Th17 mediated synovial inflammation is IL-22 independent. *Ann Rheum Dis* 2013; **72**: 1700-1707.
60. Singh S, Saraiva L, Elkington PT*, et al.* Regulation of matrix metalloproteinase-1, -3, and -9 in Mycobacterium tuberculosis-dependent respiratory networks by the rapamycin-sensitive PI3K/p70(S6K) cascade. *Faseb J* 2014; **28**: 85-93.
61. Wu Y, Zhu L, Liu L*, et al.* Interleukin-17A stimulates migration of periodontal ligament fibroblasts via p38 MAPK/NF-kappaB -dependent MMP-1 expression. *J Cell Physiol* 2014; **229**: 292-299.
62. Belton M, Brilha S, Manavaki R*, et al.* Hypoxia and tissue destruction in pulmonary TB. *Thorax* 2016; **71**: 1145-1153.
63. Domingo-Gonzalez R, Das S, Griffiths KL*, et al.* Interleukin-17 limits hypoxia-inducible factor 1alpha and development of hypoxic granulomas during tuberculosis. *JCI insight* 2017; **2**.
64. Miossec P, Kolls JK. Targeting IL-17 and TH17 cells in chronic inflammation. *Nat Rev Drug Discov* 2012; **11**: 763-776.

65. van den Berg WB, McInnes IB. Th17 cells and IL-17 a--focus on immunopathogenesis and immunotherapeutics. *Semin Arthritis Rheum* 2013; **43**: 158-170.
66. Mayer-Barber KD, Andrade BB, Oland SD*, et al.* Host-directed therapy of tuberculosis based on interleukin-1 and type I interferon crosstalk. *Nature* 2014; **511**: 99-103.

Figure Legends

Figure 1

IL-17 is expressed in granulomas of TB patients and has a divergent effect on epithelial MMP secretion in a TB network. **(A)** IL-17 is expressed around granulomas in patients with TB. The figure is representative of lung biopsies from five patients with Mtb infection (scale bar 200 μm). **(B)** Control normal lung tissue showed no immunoreactivity for IL-17 (scale bar 200 μm). (**C)** MMP-3 secretion increased 2.2-fold after stimulation with CoMTb and this was further augmented four-fold by IL-17. IL-17 also increased the baseline secretion of MMP-3 from SAECs by three-fold ($p<0.001$). **(D)** CoMTb increased MMP-9 secretion 10.5 fold ($p=0.002$), but this was suppressed by IL-17 ($p<0.0001$). **(E)** MMP-1 secretion from SAECs was augmented by 4.5-fold by CoMTb ($p<0.001$), but was not altered by IL-17. **(F)** SAECs constitutively secrete MMP-2 which was not altered significantly by CoMTb. **(G)** MMP-8 was augmented by CoMTb but only at very low concentrations.

Figure 2

MMP-3 is expressed in human respiratory epithelial cells in TB patients and MMP-3 gene expression and secretion is driven by IL-17. **(A)** Pulmonary epithelial cells adjacent to TB granulomas express MMP-3. The figure is representative of lung biopsies from five patients with TB (scale bar 20 μm). **(B)** Minimal staining for MMP-3 was observed in 5 normal lung specimens. (**C)** Kinetic experiments in NHBE cells demonstrated that MMP-3 secretion increased progressively until 72 h after stimulation with 10 ng/ml of IL-17 ($p<0.001$). **(D)** IL-17 driven MMP-3 mRNA accumulation peaked at 24 h, rising to 4-fold above baseline ($p<0.01$). **(E)** Direct infection of NHBEs with Mtb at an MOI from 0.1-10 did not alter MMP-3 secretion and there was no synergy between Mtb infection and IL-17 stimulation.

Figure 3

IL-17 and IL-22 increase TB-dependent MMP-3 secretion from fibroblasts. **(A)** CoMTb caused a concentration-dependent increment in MMP-3 secretion from MRC-5 fibroblasts ($p<0.01$). **(B)** MMP-3 full-length promoter activation in response to CoMTb was detectable at 6 h, peaking at 24 h ($p<0.001$), and thereafter remaining stable for 48 h. Results are expressed as relative luminescence (RLU) for Firefly/Renilla luciferase. **(C)** IL-17 and **(D)** IL-22 both increased CoMTb-driven MMP-3 secretion from MRC-5 fibroblasts in a concentration-dependent manner ($p<0.001$ for both cytokines), but each did not affect MMP-3 secretion as a single stimulus.

Figure 4

IL-17 and IL-22 are up-regulated in BALF from patients with TB. Concentrations of IL-17 and IL-22 were measured in BALF from 17 TB subjects and 18 well-matched respiratory symptomatic patients. **(A)** Median IL-17 concentration was increased in TB patients as compared to other respiratory symptomatic patients ($p=0.02$), although the absolute detectable concentrations were low. **(B)** Median IL-22 concentration in TB patients was 4-fold higher than in control patients ($p=0.006$) (Mann Witney U Test).

Figure 5

IL-17 regulation of MMP-3 secretion is p38 MAP kinase dependent. **(A)** Phosphorylation of p38 after 30 min of stimulation was increased by both CoMTb and IL-17. p38 phosphorylation was significantly increased when cells were co-stimulated with IL-17 and CoMTb. There was no change in total p38. Densitometric analysis was performed using Scion image software. **(B)**

MMP-3 secretion and **(C)** MMP-3 mRNA accumulation driven by IL-17 was inhibited in a concentration-dependent manner by SB203580, a specific p38 chemical inhibitor ($p<0.001$ for both protein and mRNA). **(D)** Transfection of the epithelial cells with p38 siRNA decreased IL-17/CoMTb driven MMP-3 secretion by 50% ($p<0.01$). The suppression was maximal with 30 nM of siRNA **(E)** Similarly IL-17 driven MMP-3 mRNA decreased to baseline by siRNA inhibition of p38 ($p<0.01$). Cells were also transfected with non-targeting (NT) siRNA, which had no effect.

Figure 6

Epithelial MMP-3 secretion is regulated by the PI3K p110α subunit and AKT. **(A)** IL-17-dependent MMP-3 secretion was reduced to baseline after incubation of NHBEs with LY294002, a non-specific PI3-Kinase proximal subunit inhibitor (Figure 6A, $p<0.0001$). Suppression was maximal at 10 μM. **(B)** siRNA transfection of NHBEs identified that the p110α subunit was key in this suppression (Figure 6B, $p<0.0001$). MMP-3 mRNA was suppressed to baseline with 30 nM of siRNA. Cells were also transfected with non-targeting (NT) siRNA, which had no effect. **(C)** Downstream, inhibition of AKT by a specific inhibitor (AKT inhibitor VIII) resulted in MMP-3 suppression to baseline. The effect was dose-dependent and maximal at 2.5 μM of the AKT inhibitor (Figure 6C, $p<0.0001$).

SUPPLEMENTARY MATERIAL ONLINE

Supplementary materials and methods: YES

Supplementary figure legends: YES

Figure S1. Transfection efficiency was confirmed with siGLO

Figure S2. Positive and negative controls for IL-17 immunohistochemistry

Figure S3. IL-17 driven MMP-3 secretion in both SAEC and NHBE cells was concentration-dependent but TIMP-1/-2 were unaffected

Figure S4. Epithelial MMP-3 and MMP-9 were not driven by IL-22 or IL-23

Figure S5. TNF-α did not drive MMP-3 from NHBE cells

Figure S6. IL-23 was not detectable in TB BALF

Figure S7. siRNA-mediated knockdown of p38 and PI3K p110α was confirmed by phospho-western analysis and mRNA expression

Table S1. Cytokine and chemokine concentrations in the culture medium of normal human bronchial epithelial cells stimulated with CoMTb or CoMTb+IL-17

Table S2. Cytokine and chemokine concentrations in the culture medium of monocytes stimulated with CoMCont or CoMTb

Materials and Methods

Reagents

General laboratory reagents were purchased from Sigma, Poole, UK and Invitrogen, Paisley, UK. Mtb culture reagents were purchased from BD Biosciences, Oxford, UK. Inhibitory chemicals SB203580 (p38 inhibitor), LY294002 (PI3K inhibitor), AKT inhibitor VIII (AKT inhibitor) and phospho- and total-p38 antibodies were purchased from Merck Chemicals Ltd, Nottingham, UK. Recombinant human IL-17, IL-22, and TNF-α were purchased from Peprotech, London, UK. Ficoll Paque and the ECL system were purchased from Amersham Biosciences, Little Chalfont, UK. All siRNA oligonucleotides and reagents were purchased from ThermoScientific Dharmacon, Northumberland, UK.

Immunohistochemical analysis of patient biopsies

Ethical consent for the use of archived lung biopsies was obtained from the Hammersmith Hospitals Research Ethics Committee. Immunohistochemistry was performed on paraffin embedded lung biopsies from 5 patients with culture-proven Mtb infection and 5 uninfected controls. Sections of 4 μm thickness were de-waxed with 3 changes of xylene followed by 3 changes of alcohol, before being rehydrated. Endogenous peroxidase activity was blocked with 0.6% hydrogen peroxide for 15 min. Antigen retrieval was performed by microwaving the sections for 20 min in citrate buffer (0.01M citrate pH 6.0). Non-specific binding was blocked with 5% normal goat serum for 10 minutes. The primary antibodies were applied in 0.01M PBS / azide / BSA for 1 h at room temperature. After 3 rinses in PBS, the antibody was detected with the Menarini non-biotinylated kit according to manufacturer's instructions. Peroxidase activity was developed with diaminobenzidine (DAB, Menarini). Slides were counterstained

with Coles haematoxylin, dehydrated and mounted. Antibodies for MMP-3 and IL-17 were purchased from Abcam, Cambridge, UK (catalogue numbers ab137659 and ab9565 respectively). The antibodies were both polyclonal rabbit and had a human-specific reactivity.

Clinical study

BALF samples were collected from patients being routinely investigated for respiratory symptoms at Nalanda University Hospitals, Patna, India. The study was approved by the ethics review board at Nalanda Medical College and University Hospitals (Reference Number SS/0810/TB). To limit user and procedure variability, bronchoscopy was performed by one of two bronchoscopists using flexible bronchoscopes. Samples that were Mtb culture positive were stored at -20 °C. Exclusion criteria from the study were a previous history of TB (to decrease likelihood of multi- and extensively drug resistant (MDR/ XDR) cases), age <18 years, severe chronic lung disease, malignancy, positive HIV status, exposure to corticosteroids or immunosuppressive drugs, or inability to consent. Samples were centrifuged to remove cellular debris, and then sterile filtered through a 0.2 μm Durapore membrane (Millipore, Nottingham, East Midlands, UK) to remove Mtb from the samples. This does not interfere with detection of cytokines. IL-17 concentration was measured with a Bioplex Luminex 200 (Biorad Laboratories Ltd, Hemel Hempstead, UK) and IL-22 with an ELISA kit (R&D Systems Europe, Abingdon, Oxford, UK).

Mtb Culture and generation of TB medium

M.tuberculosis H37Rv was were cultured in Middlebrook 7H9 medium supplemented with 10% albumin, dextrose-catalase enrichment medium, 0.2% glycerol and 0.02% Tween-80 with agitation. Culture growth was monitored with a Biowave cell density meter (WPA, Cambridge) and the MTb was sub-cultured when the optical density exceeded 1.00. For infection

experiments, culture at mid log growth at an optical density of 0.60 was used, which corresponded to 1 x 10^8 – 2 x 10^8 colony forming units (CFU) per ml, within a 2-fold error. Optical density was correlated with CFU by performing colony counts in triplicate on Middlebrook 7H11 agar supplemented with OADC enrichment medium and 0.5% glycerol. The amebocyte lysate assay (Associates of Cape Cod, East Falmouth, MA, USA) was used to assay the endotoxin level of the MTb culture and this was found to be less than 0.3 ng/ml lipopolysaccharide.

Monocyte purification

Monocytes used in the experiments were from two donor buffy coats, from the National Blood Transfusion Service, Colindale, London. The leukocytes were mixed 50:50 with Hanks' Balanced Salt Solution (HBSS), layered onto Ficoll Paque (Amersham Biosciences, Little Chalfont, UK) and centrifuged at 480 rcf for 30 min. The mononuclear cell layer was removed and then washed a total of five times in HBSS, spinning down the cell pellet at 308 rcf after each wash. Total monocytes were calculated by counting the number of adherent cells in a Neubauer counting chamber after incubation for 5 min at 37 ^{o}C. Monocytes were plated in at 250,000 monocytes /cm^2 diluted in RPMI 1640. After one hour, non-adherent cells were removed by washing three times with HBSS, then the media was replaced with RPMI 1640 supplemented with 2 mM glutamine and 10 μg/ml ampicillin. Monocyte purity was assessed using two colour fluorescence activated cell scanning (FACS) for anti-CD3 (fluorescein isothiocyanate, FITC, BD Pharmingen, Oxford, UK) and anti-CD14 (phyco erythrin, PE, BD Pharmingen, Oxford, UK) and analysed on a BD FACSCaliber flow cytometer. Monocyte purity was over 95%, with less than 5% cells CD3 positive.

Monocyte and epithelial cell infection protocol

Monocytes were cultured in RPMI with 2 mM glutamine and 10 μg/ml ampicillin (which has been shown not to inhibit the growth of mycobacteria at this concentration). Monocytes were infected immediately after the completion of adhesion purification, using Mtb at an OD of 0.60 to calculate the correct multiplicity of infection (MOI). Mtb was sonicated for 30 s prior to infection to minimise clumping. Trypan blue exclusion was used to compare cell viability in un-infected and infected monocytes at 24 h and no differences were observed.

For epithelial cell infections, media was changed at the start of the experiment and Mtb added at the appropriate MOI. Cells were then washed after 2 h to remove non-adherent bacilli, and fresh culture medium added. Ziehl-Nielsen staining demonstrated that 30% cells were infected at 6 hours at an MOI of 10, which is similar to reports of A549 infection rates. Mtb was removed by filtration through a 0.2μM Durapore membrane.

Generation of CoMTb

Cell culture medium was harvested at 24 h. Medium was spun at 13,000 rcf to remove cellular debris, and then sterile filtered through a 0.2 μm Anopore membrane. Colony counting on Middlebrook 7H11 agar showed no viable bacteria in CoMtb. Medium from infected monocytes was termed conditioned medium from monocytes infected with Mtb (CoMTb). With each batch of CoMTb that was generated, supernatants are also collected from uninfected monocytes (CoMCont). A comparative analysis of the cytokines and chemokines in CoMCont and CoMTb has been performed previously using the Luminex Bead Multi-Analyte Profiling facility. Monocytes infected with Mtb consistently secrete more cytokines and chemokines that uninfected monocytes (supplementary material, Table S2). Donor related variability in the cytokine and chemokine profiles of CoMTb was within statistically acceptable limits. Both CoMCont and CoMTb were used at a dilution of 1 in 5 (with the cell culture medium) in 12- or 24-well plates.

Cell culture

Primary small airway epithelial cells (SAEC) and primary normal human bronchial epithelial cells (NHBE) were purchased from Lonza Biosciences, Basel, Switzerland. Cells had been acquired bronchoscopically from healthy male adult volunteers. Each frozen ampoule contained ~0.5-1 x 10^6 cells. Cells were initially propagated in a T25 flask until they reached 70–80% confluence. On subsequent subculture, flasks were seeded at 3,500 cells/cm^2 density and after the final subculture, cells were seeded at a density of 1.5×10^3 cells/cm^2 in a 12- or 24-well plate in fresh medium. Cells were cultured in bronchial epithelial growth media according to the supplier's instructions. All experiments were performed between passages 4 and 5. For subculture, medium was aspirated, the cell monolayer was washed with hydroxyethyl piperazine ethanesulfonic acid (HEPES) solution, trypsin was added for 5 minutes and then neutralized with trypsin neutralising solution.

The human MRC-5 fibroblast line was grown in Eagle's medium with 10% fetal calf serum (FCS) and subcultured when cells were 70-80% confluent as per suppliers' instructions (Sigma-Aldrich, Gillingham, Dorset, UK). Adherent cells were washed with PBS and then detached from the surface with 0.25% Trypsin-ethylenediaminetetraacetic acid (EDTA) solution. Cells were re-suspended in fresh media at a seeding density of $2\text{-}4\times10^4$ cells/cm^2. For experiments, $1\text{-}2\times10^4$ cells/cm^2 were seeded in a 24-well plate in fresh medium with 1% FCS and stimulated at 70-80% confluence.

Experimental design

When epithelial the cells were 80% confluent, they were stimulated with a 1 in 5 dilution of Conditioned Medium from Monocytes infected with Mtb (CoMTb), as previous studies had

shown maximal MMP response at this dilution. For MRC-5 cells, CoMTb was used at a 1 in 50 dilution. Cells were pre-treated for 2 h with chemical inhibitors which were used at the concentrations specified in the graphs. The inhibitors were dissolved in dimethyl sulfoxide (DMSO) which was also added to the control wells (maximal final concentration 0.1%). After the use of CoMTb and inhibitors, the viability of cells was confirmed and no difference were observed in cells treated with inhibitor.

Supernatants were harvested at 72 h after stimulation for MMP secretion analysis and mRNA extraction was performed at 24 h after stimulation. For kinetic experiments, supernatants or RNA extraction was performed at 0, 24, 48, 72 and 96 h. Supernatants were spun at 11,700 rcf for 5 min to remove cellular debris, then frozen at -20 °C. Baseline levels of MMPs in the conditioned media used to stimulate cells was negligible compared to the concentrations secreted by the stimulated cells as the CoMCont and CoMTb was taken from monocytes at 24 h, whereas monocyte MMP secretion increases from 48 h and peaks at 72 h.

Measurement of MMP and TIMP concentrations

MMP-1, -3, -9 and TIMP-1, -2 concentrations in cell culture medium were measured by ELISA according to the manufacturer's instructions (Catalogue number MMP300, R&D Systems Europe, Abingdon, Oxford, UK). The lower level of detection was 30 pg/ml. MMP-1, -3 and -9 concentrations were also analysed using a Fluorokine multianalyte profiling kit according to the manufacturer's protocol (R&D Systems Europe, Abingdon, Oxford, UK) on the Luminex platform (Bio-Rad Laboratories Ltd, Hemel Hempstead, UK). The minimum level of detection for MMPs was 10 pg/ml.

Gelatin zymography

MMP-9 gelatinolytic activity was detected by zymography using standard methodology. In brief, standards and cell culture supernatants were loaded with 5 x loading buffer : (0.25 M Tris (pH 6.8), 50% glycerol, 5% sodium dodecyl sulphate (SDS) and bromophenol blue) and run on 11% acrylamide gels impregnated with 0.1% gelatin as substrate. After 3.5 h at 180 V (buffer 25 mM Tris, 190 mM glycine, and 0.1% SDS), the gel was renatured in 2.5% Triton X for 1 h with agitation. After two washes in collagenase buffer (55 mM Tris base, 200 mM sodium chloride, 5 mM calcium chloride, and 0.02% Brij, pH 7.6), gels were incubated overnight in fresh collagenase buffer at 37 °C. Gelatinolytic activity was detected using 0.02% Coomassie blue in 1:3:6 acetic acid: methanol: water. All experimental samples were run in parallel with 2 ng recombinant MMP-9 standard (Merck, Chemicals Ltd, Nottingham, UK). Digital image acquisition (UVP, Ultraviolet Products) of the bands was followed by densitometric analysis using the image processing software, Scion Image (downloaded from Scion Corporation Scientific Computing, Frederick, Maryland, USA).

Promoter-reporter assay

Promoter-reporter studies were performed using FuGENE® HD Transfection Reagent from Roche Applied Sciences (purchased from Sigma-Aldrich, Gillingham, Dorset, UK) and Promega's Dual-Luciferase™ Reporter (DLR™) Assay System (Promega UK, Southampton, UK). The MMP-3 promoter (1206 base pairs) linked to firefly luciferase in pGL4 basic vector (Promega) and the reference gene thymidine kinase promoter linked to *Renilla* luciferase in the pRL control vector (pRL-TK; Promega) were generated. MRC-5 fibroblasts were grown overnight in a 12-well plates (3.8 cm^2/well) at a recommended seeding density of 100,000 cells/well so that the monolayer was 80-90% confluent at the time of transfection. A 6:2 ratio of transfection reagent (37.6 µl/well) to purified plasmid DNA (1.6 µg/well) and pRL-TK (0.16

µg/well) was used according to manufacturer's instructions. Plasmid DNA purity and concentration had been estimated using a 260 nm/280 nm absorbance ratio; the optimal ratio being 1.8. Fibroblasts were stimulated with 10% CoMTb and harvested at given time intervals (0, 6, 24 and 48 h). Cells were washed twice with sterile PBS prior to using 100 µl of passive lysis buffer from the DLR™ Assay kit (Promega). Luminescence was detected using the Promega Dual Luciferase Assay system. *Renilla* luciferase activity was used to normalize firefly activity in order to control for transfection efficiency. Results were expressed as relative luminescence (RLU) for Firefly/Renilla luciferase (ratio of luminescence for MMP-3 promoter to that of thymidine kinase promoter).

Phospho-western analysis

NHBE cells were stimulated in 6-well plates and at specific time points, cells were washed with sterile phosphate buffered saline (PBS), lysed with 100 µl SDS sample buffer (62.5 mM Tris [pH 6.8], 2% SDS, 10% glycerol, 50 mM dithiothreitol (DTT), and 0.01% Bromophenol blue), transferred to cold microtubes and frozen at -80 ºC. Forty-µL samples were mixed with 40 µl loading buffer (10% glycerol, 5% 2-mercaptoethanol, 2% SDS, 0.06 M Tris pH 6.8, Bromophenol blue) and heat inactivated at 100 ºC for ~2 min prior to separation on 10% acrylamide gels. Molecular weight markers (Amersham Biosciences, Little Chalfont, UK) were run concurrently. Subsequently, proteins were electro-transferred to a nitrocellulose membrane (Amersham Biosciences, Little Chalfont, UK) which was blocked for 1 h with agitation in 5% milk protein (Marvel, Nestlé) mixed with 0.1% Tween-20. The membrane was probed with a primary antibody by incubating at 4 °C and next day the membrane was washed 3 times and incubated for 1 h with HRP-linked goat anti-rabbit IgG secondary antibody. Luminescence was then detected with the ECL system according to the manufacturer's protocol (Sigma-Aldrich, Gillingham, Dorset, UK).

Small interfering (siRNA) transfection

All siRNA oligonucleotides and reagents were purchased from ThermoScientific Dharmacon (Northumberland, UK). The siRNAs were purchased as double stranded, chemically synthesized oligonucleotides in a smart pool, targeting the transcription products from 4 alleles of the gene of interest. For reconstitution, the siRNA was dissolved in a special buffer, mixed on a shaker for 30 min, aliquoted and then stored at -80 °C.

Prior to planning the individual experiments, the conditions were optimised using a transfection control. The transfection control, siGLO (Green), confirms localisation to the nucleus and optimal delivery of the siRNA in the cell type being investigated. It is an oligonucleotide labelled with a fluorophore on the sense strand. Supplementary material, Figure S1 illustrates the 72.45% transfection achieved in NHBEs with siGLO at 30 nM in a 1:1 ratio with Lipofectamine. A negative control of non-targeting sequences was incorporated in all experiments to distinguish sequence specific silencing from non-specific effects of siRNA. In brief, 12-well plates were seeded with NHBEs at 150,000 cells per well the day before experiments. Lipofectamine was used at 25 μg/ml per well, and siRNA at 10–30 nM per well. Lipofectamine and siRNA were allowed to complex in a 1:1 ratio (by volume) at room temperature for 20 min. The mixture was then added to cells with the basal medium for 4 h. Cells were then washed, rested for an additional 4 hohurs and then stimulated. Samples were collected at the end of the experiment.

RNA extraction, cDNA synthesis and Reverse Transcription – quantitative polymerase chain reaction (RT-qPCR)

RNA extraction was performed using the Qiagen RNeasy Minikit according to manufacturer's instructions (Qiagen, Manchester, UK). RNA was eluted with RNase-free water and stored at -

80 °C. cDNA synthesis was performed using the Quantitect reverse transcription kit. RNA was quantified on a Nanodrop spectrophotometer. A volume of RNA equivalent to 1µg was diluted to 12 µl with RNase-free water. Two µl of genomic (g) DNA wipeout buffer was added to each sample. Samples were then heated at 42 ˚C for 2 min. Six-µl of the reverse transcription mastermix was added to each sample, before heating again at 42 °C for 15 min, followed by 95°C for 3 min. The resulting cDNA was stored at -20 °C. Real time quantitative PCR was performed using Brilliant II QPCR master mix (Stratagene, Cambridge, UK) on the Stratagene Mx3000P platform. MMP primers and probes were as described previously. The C_T at which amplification entered the exponential phase was determined. A lower C_T indicates a higher quantity of starting RNA. To determine the relative RNA levels within samples, standard curves were prepared by making five-fold serial dilutions of each sample. Standard curves for C_T versus input RNA were prepared, and relative quantities of starting RNA in each sample were determined. Experimental MMP data was normalized to three reference RNA namely, *GAPDH*, *18S* ribosomal RNA and cyclophilin A (*PPIA*), whose C_T values remained stable under different experimental conditions. Analysis of MMP mRNA expression was first undertaken by the standard curve method, and results were corroborated by using the C_T values to assess levels of gene expression.

Statistical analysis

Data is presented as mean ± SD and represent experiments performed in triplicate on at least two occasions, unless stated otherwise. Paired groups were compared with Student's *t*-test. Multiple intervention experiments were compared by two-way ANOVA, with Tukey's correction for multiple pairwise comparisons. BALF MMP concentrations were compared using the Mann Witney U test. A p value of <0.05 was taken as statistically significant. In figures,

$p<0.05$ is illustrated with *, $p < 0.01$ with **, $p < 0.001$ with *** and $p < 0.0001$ with ****. All secretion and mRNA expression data shown here are representative of 3 separate experiments.

Supplementary Figure Legends

Figure S1. Transfection efficiency was confirmed with siGLO

72.45% transfection of NHBEs was achieved with siGLO, the transfection control. The dot plot figure demonstrates the upper right and left quadrants only.

Figure S2. Positive and negative controls for IL-17 immunohistochemistry

(A) As a positive control, colonic T lymphocytes showed a strong staining for IL-17 (scale bar 200 μm). **(B)** No staining was seen when a secondary antibody only was used as a negative control (scale bar 100 μm).

Figure S3. IL-17 driven MMP-3 secretion in both SAEC and NHBE cells was concentration-dependent but TIMP-1/-2 were unaffected

(A) SAECs were stimulated with increasing concentrations of IL-17. MMP-3 secretion peaked at 30 ng/ml of IL-17, after which it remained unchanged. There was a concentration-dependent increment in MMP-3 concentration from a baseline of 145.6±9.9 pg/ml to a maximal concentration of 1575.4±91.44 pg/ml when the cells were stimulated with 30 ng/ml of IL-17. **(B)** IL-17 did not significantly alter the baseline or CoMTb-dependent TIMP-1 suppression from SAECs. **(C)** TIMP-2 secretion was also unaffected by CoMTb or IL-17. **(D)** NHBE cells were stimulated with increasing concentrations of IL-17. MMP-3 secretion peaked at 10 ng/ml

of IL-17. There was a concentration-dependent increment in MMP-3 concentration from a baseline of 155.6±10.4 pg/ml to a maximal concentration of 1462.4±292 pg/ml when the cells were stimulated with 10ng/ml of IL-17.

Figure S4. Epithelial MMP-3 and MMP-9 were not driven by IL-22 or IL-23

(A) MMP-3 secretion from NHBE's was unaffected by IL-22 and also by **(B)** IL-23. **(C)** MMP-9 secretion was also unaltered by IL-22 and **(D)** by IL-23. These were investigated over a concentration range of 1-30 ng/ml in a TB network.

Figure S5. TNF-α did not drive MMP-3 from NHBE cells

Stimulation of NHBE cells with TNF-α (concentration range 1–20 ng/ml) in combination with IL-17 did not drive MMP-3. TNF-α alone at a maximal dose of 20 ng/ml also did not drive MMP-3.

Figure S6. IL-23 was not detectable in TB BALF

IL-23 was not detectable in the majority of BALF samples from TB and control subjects (n=17 for TB patients, n=18 for well-matched controls).

Figure S7. siRNA-mediated knockdown of p38 and PI3K p110α was confirmed by phospho-western analysis and mRNA expression

(A) On phospho-western analysis of p38 in NHBE's, CoMTb and IL-17-mediated activation was abrogated by p38 specific siRNA. A concentration-dependent response was observed and no activity was seen at 30 nM of the siRNA. **(B)** Total p38 mRNA levels were suppressed to

below baseline when the NHBE's were incubated with the p38 specific siRNA in a concentration-dependent manner. **(C)** On phospho-western analysis of PI3K p110α in NHBE's, CoMTb and IL-17 mediated activation was abrogated with the specific siRNA. A concentration-dependent response was again observed and was complete with 30 nM. **(D)** Total p110α mRNA levels were suppressed to below baseline when the NHBE's were incubated with the p110α-specific siRNA. Non-targeting siRNA had no effect.

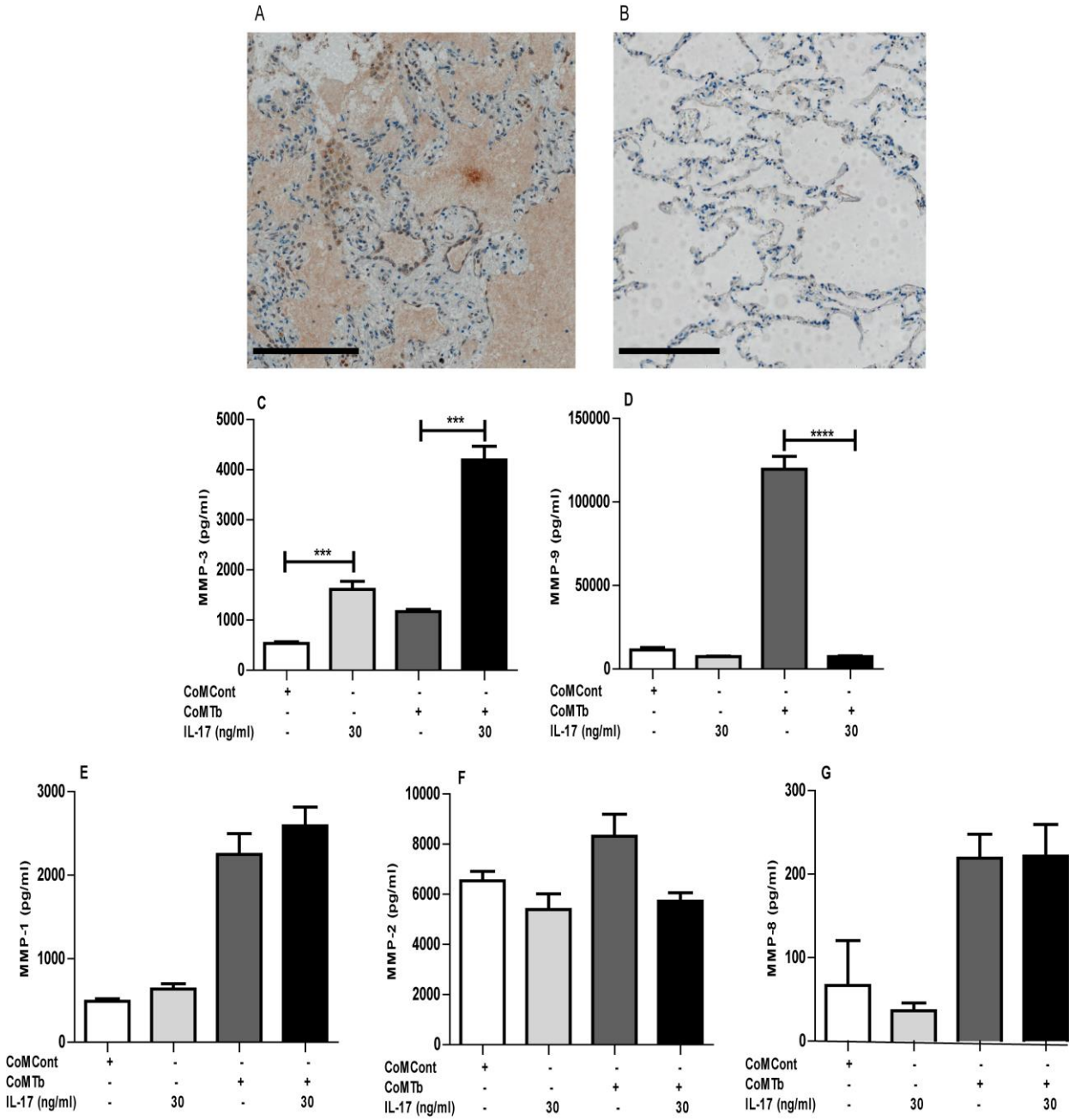
A
B
C
MMP-3 (pg/ml)
5000
4000
3000
2000
1000
0
***
***
CoMCont + - - -
CoMTb - - + +
IL-17 (ng/ml) - 30 - 30
D
MMP-9 (pg/ml)
150000
100000
50000
0
****
CoMCont + - - -
CoMTb - - + +
IL-17 (ng/ml) - 30 - 30
E
MMP-1 (pg/ml)
3000
2000
1000
0
CoMCont + - - -
CoMTb - - + +
IL-17 (ng/ml) - 30 - 30
F
MMP-2 (pg/ml)
10000
8000
6000
4000
2000
0
CoMCont + - - -
CoMTb - - + +
IL-17 (ng/ml) - 30 - 30
G
MMP-8 (pg/ml)
300
200
100
0
CoMCont + - - -
CoMTb - - + +
IL-17 (ng/ml) - 30 - 30

Figure 1

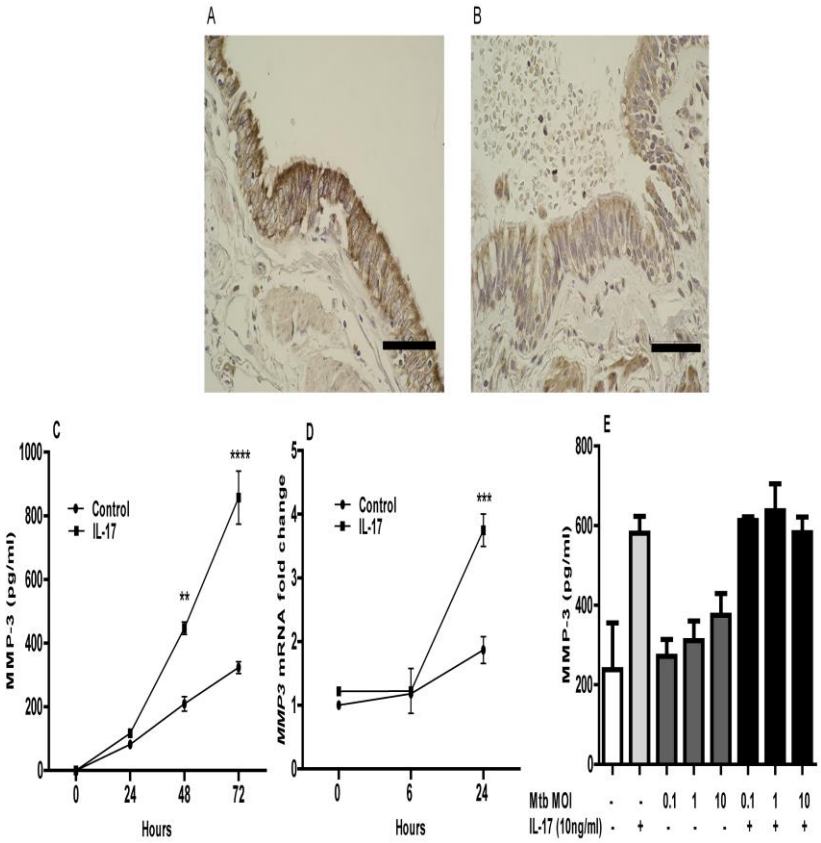
A
B
C
MMP-3 (pg/ml)
Control
IL-17
****
**
Hours
D
MMP3 mRNA fold change
Control
IL-17
***
Hours
E
MMP-3 (pg/ml)
Mtb MOI
IL-17 (10ng/ml)

Figure 2

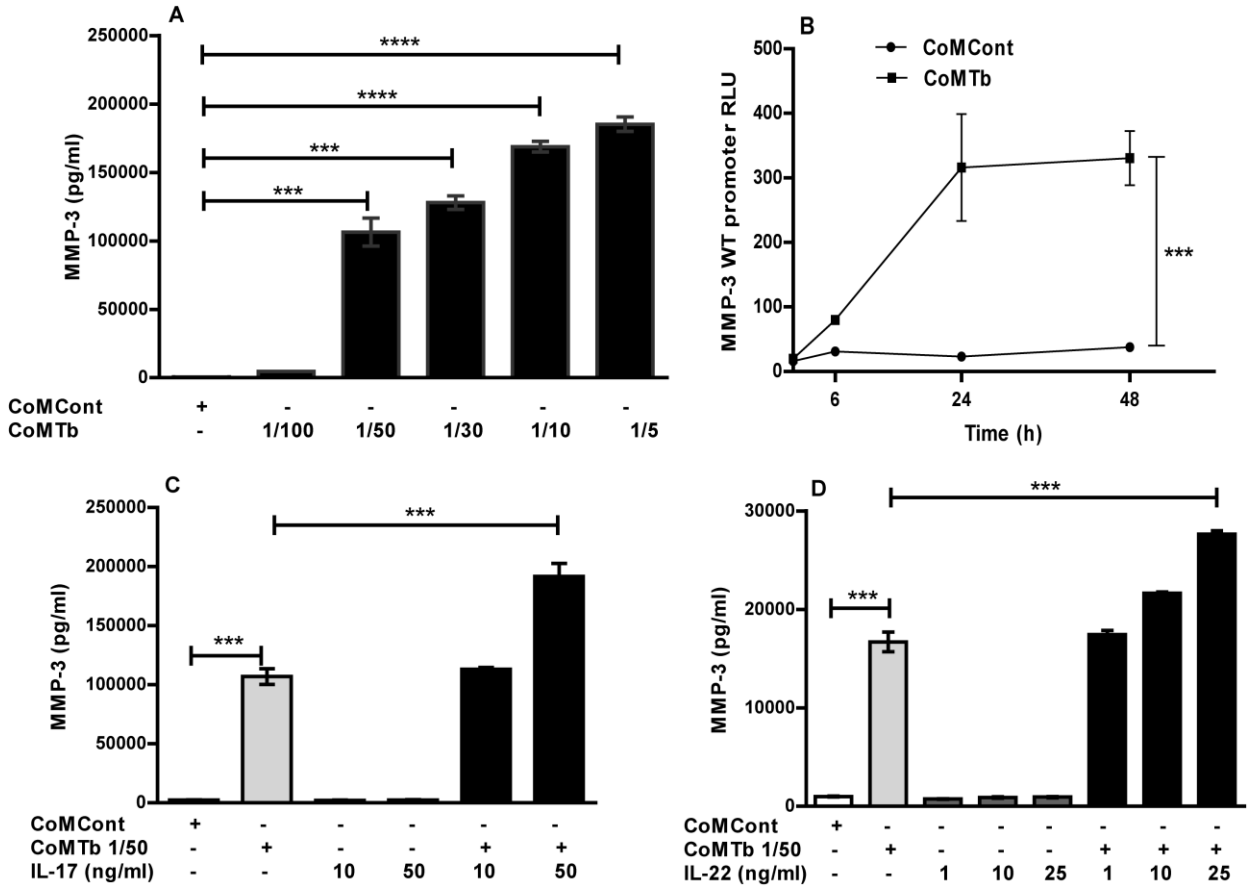
A
MMP-3 (pg/ml)
250000
200000
150000
100000
50000
0
****
****
***
***
CoMCont + - - - - -
CoMTb - 1/100 1/50 1/30 1/10 1/5
B
CoMCont
CoMTb
MMP-3 WT promoter RLU
500
400
300
200
100
0
***
6
24
48
Time (h)
C
MMP-3 (pg/ml)
250000
200000
150000
100000
50000
0
***
***
CoMCont + - - - - -
CoMTb 1/50 - + - - + +
IL-17 (ng/ml) - - 10 50 10 50
D
MMP-3 (pg/ml)
30000
20000
10000
0
***
***
CoMCont + - - - - - - -
CoMTb 1/50 - + - - - + + +
IL-22 (ng/ml) - - 1 10 25 1 10 25

Figure 3

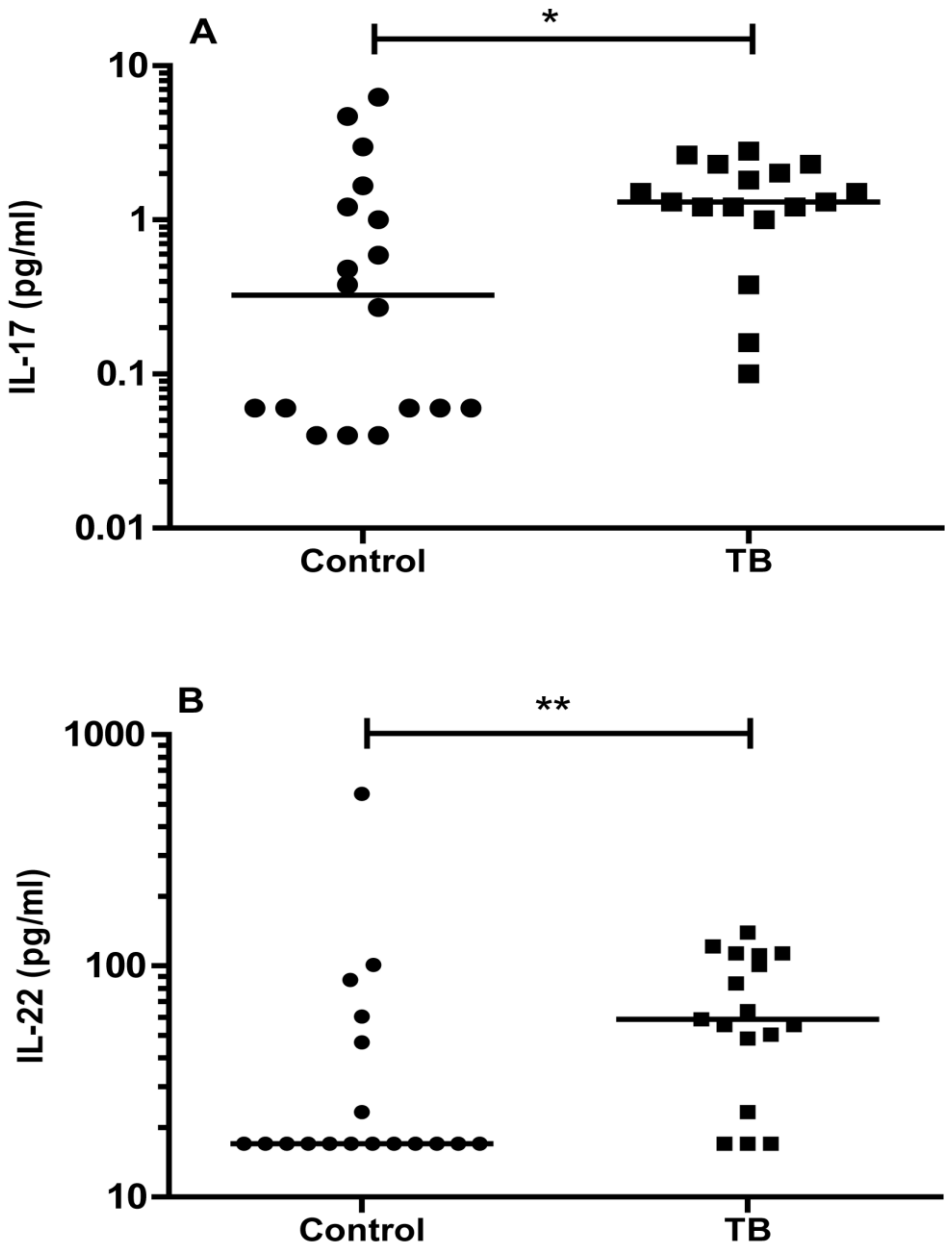
A
*
10
1
0.1
0.01
IL-17 (pg/ml)
Control
TB
B
**
1000
100
10
IL-22 (pg/ml)
Control
TB

Figure 4

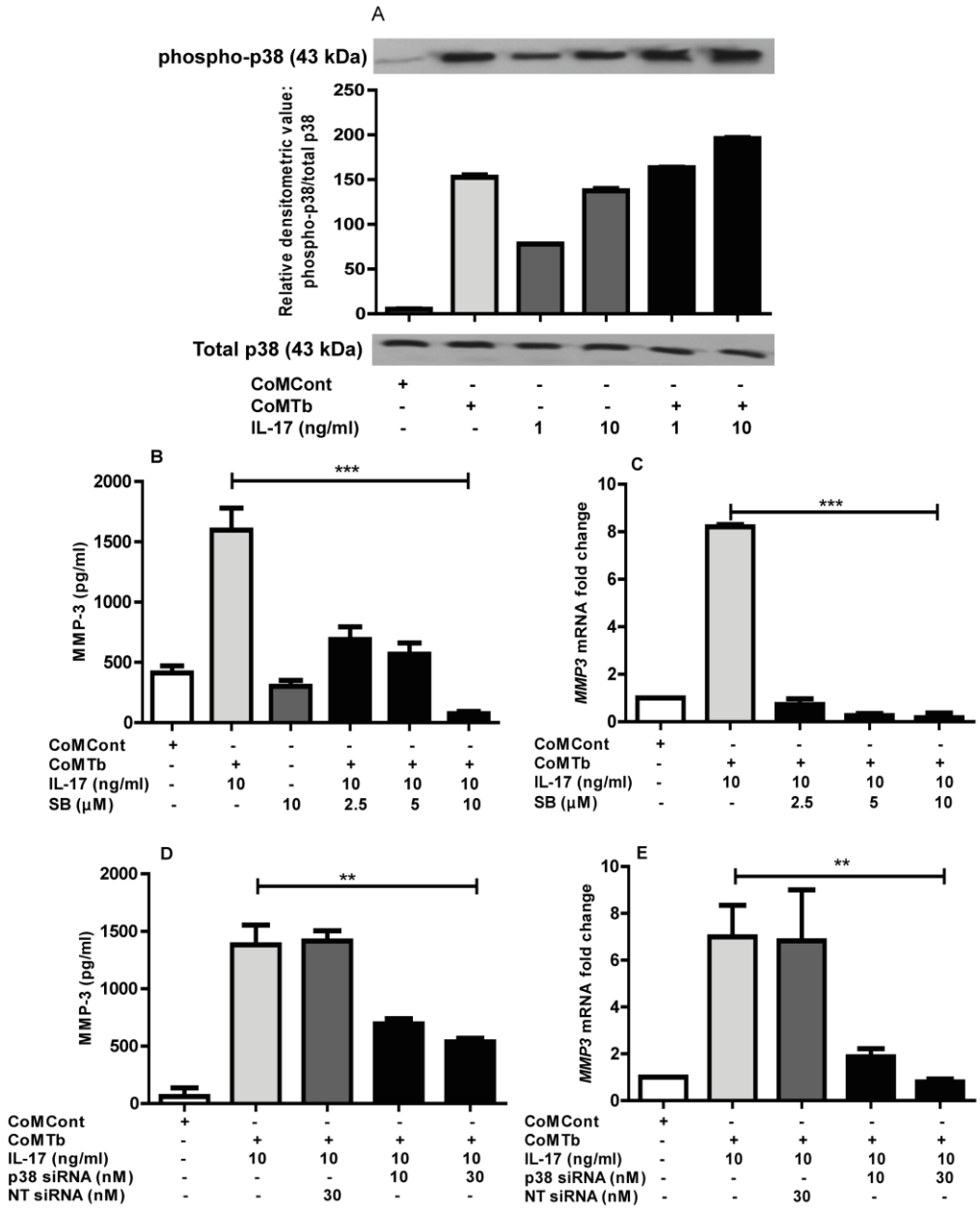
A
phospho-p38 (43 kDa)
Relative densitometric value: phospho-p38/total p38
250
200
150
100
50
0
Total p38 (43 kDa)
CoMCont + - - - - -
CoMTb - + - - + +
IL-17 (ng/ml) - - 1 10 1 10
B
MMP-3 (pg/ml)
2000
1500
1000
500
0
***
CoMCont + - - - - -
CoMTb - + - + + +
IL-17 (ng/ml) - 10 - 10 10 10
SB (µM) - - 10 2.5 5 10
C
MMP3 mRNA fold change
10
8
6
4
2
0
***
CoMCont + - - - -
CoMTb - + + + +
IL-17 (ng/ml) - 10 10 10 10
SB (µM) - - 2.5 5 10
D
MMP-3 (pg/ml)
2000
1500
1000
500
0
**
CoMCont + - - - -
CoMTb - + + + +
IL-17 (ng/ml) - 10 10 10 10
p38 siRNA (nM) - - - 10 30
NT siRNA (nM) - - 30 - -
E
MMP3 mRNA fold change
10
8
6
4
2
0
**
CoMCont + - - - -
CoMTb - + + + +
IL-17 (ng/ml) - 10 10 10 10
p38 siRNA (nM) - - - 10 30
NT siRNA (nM) - - 30 - -

Figure 5

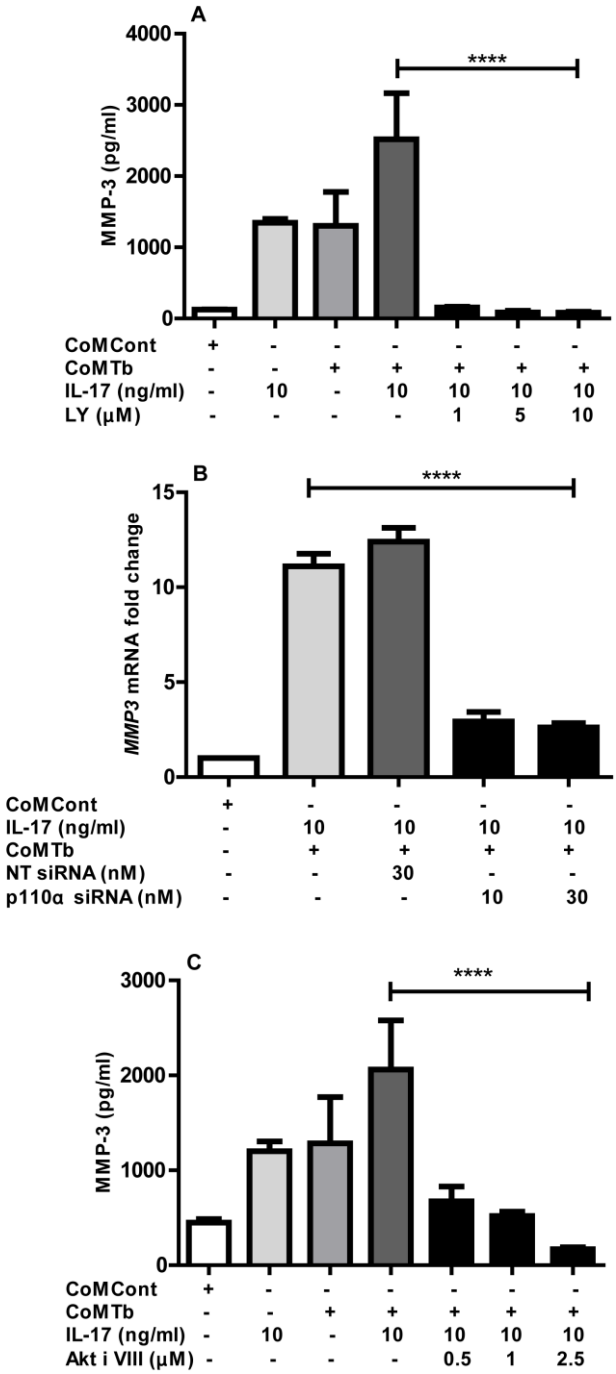
A
MMP-3 (pg/ml)
4000
3000
2000
1000
0
****
CoMCont + - - - - - -
CoMTb - - + + + + +
IL-17 (ng/ml) - 10 - 10 10 10 10
LY (µM) - - - - 1 5 10
B
MMP3 mRNA fold change
15
10
5
0
****
CoMCont + - - - -
IL-17 (ng/ml) - 10 10 10 10
CoMTb - + + + +
NT siRNA (nM) - - 30 - -
p110α siRNA (nM) - - - 10 30
C
MMP-3 (pg/ml)
3000
2000
1000
0
****
CoMCont + - - - - - -
CoMTb - - + + + + +
IL-17 (ng/ml) - 10 - 10 10 10 10
Akt i VIII (µM) - - - - 0.5 1 2.5

Figure 6

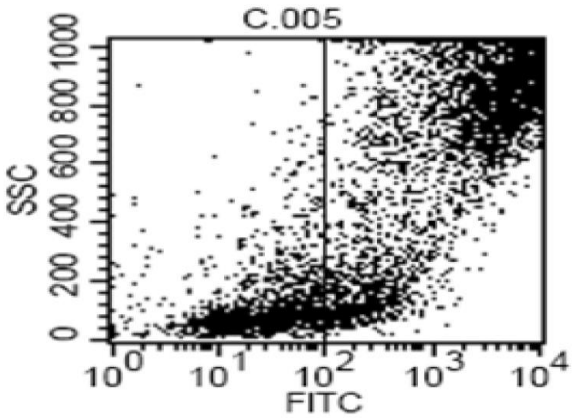

Quad	% Total
UL	27.55
UR	72.45
LL	0.00
LR	0.00

Figure S1

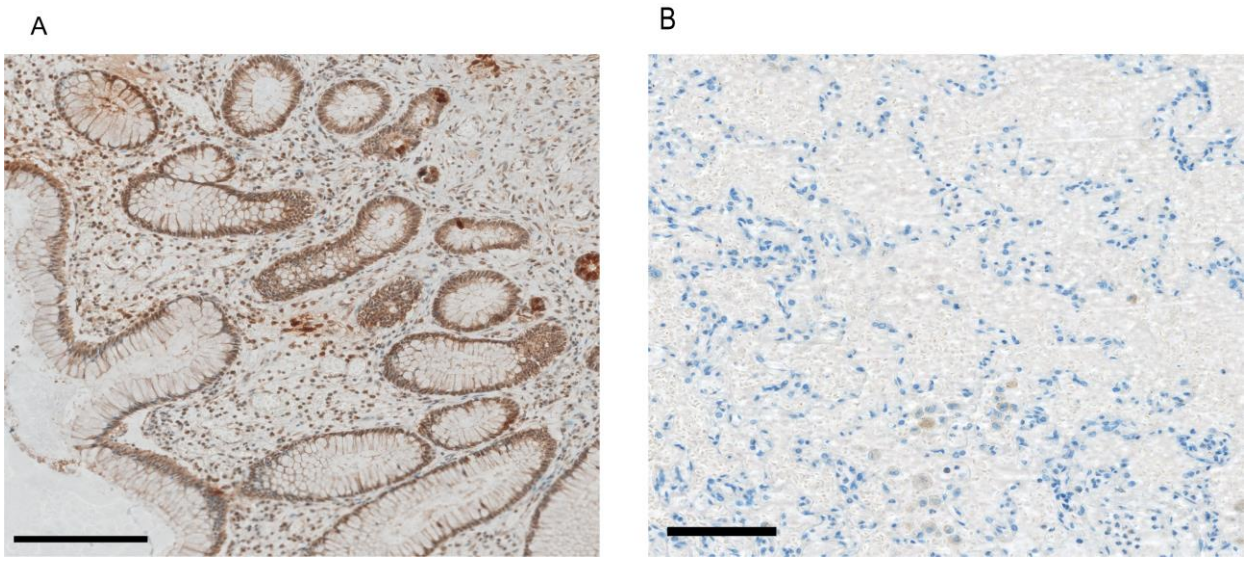

Figure S2

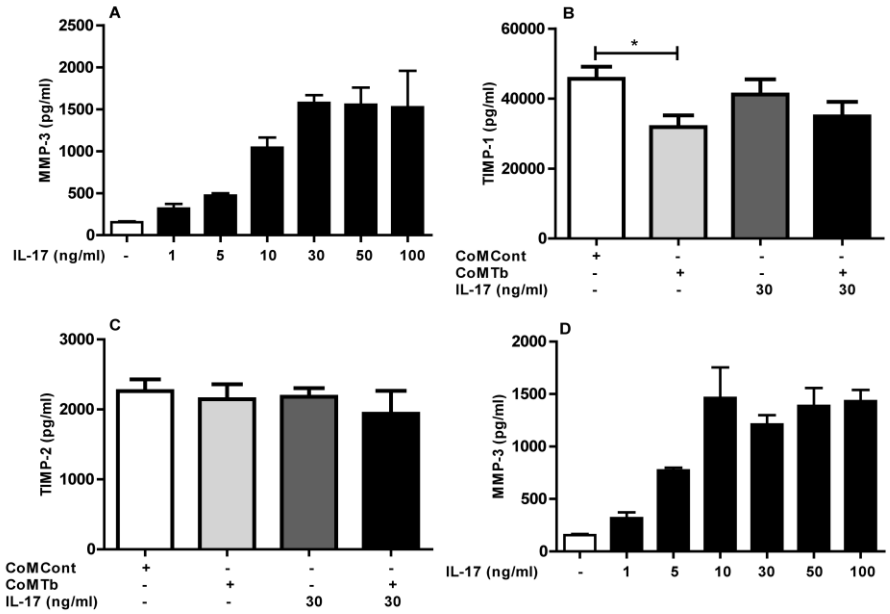
A
MMP-3 (pg/ml)
2500
2000
1500
1000
500
0
IL-17 (ng/ml) - 1 5 10 30 50 100
B
TIMP-1 (pg/ml)
60000
40000
20000
0
*
CoMCont + - - -
CoMTb - + - +
IL-17 (ng/ml) - - 30 30
C
TIMP-2 (pg/ml)
3000
2000
1000
0
CoMCont + - - -
CoMTb - + - +
IL-17 (ng/ml) - - 30 30
D
MMP-3 (pg/ml)
2000
1500
1000
500
0
IL-17 (ng/ml) - 1 5 10 30 50 100

Figure S3

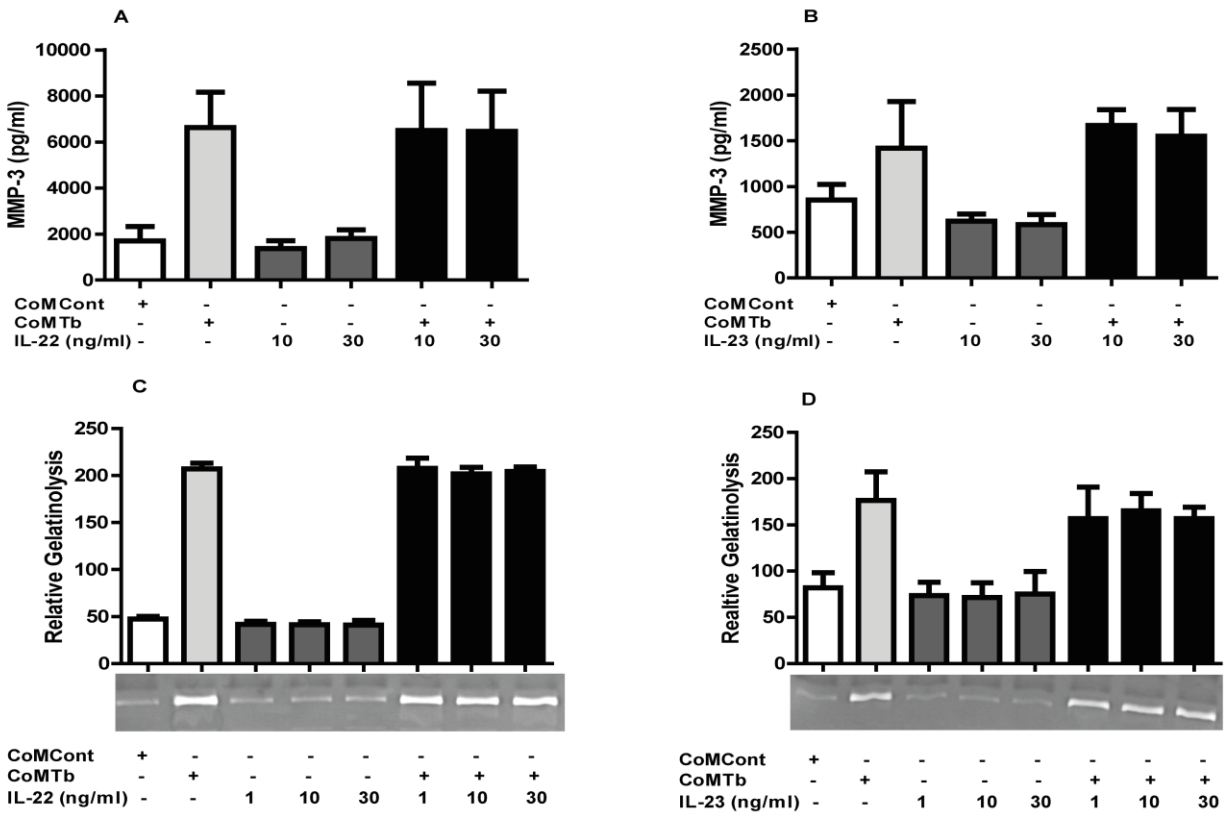
A
MMP-3 (pg/ml)
10000
8000
6000
4000
2000
0
CoMCont + - - - - -
CoMTb - + - - + +
IL-22 (ng/ml) - - 10 30 10 30
B
MMP-3 (pg/ml)
2500
2000
1500
1000
500
0
CoMCont + - - - - -
CoMTb - + - - + +
IL-23 (ng/ml) - - 10 30 10 30
C
Relative Gelatinolysis
250
200
150
100
50
0
CoMCont + - - - - - - -
CoMTb - + - - - + + +
IL-22 (ng/ml) - - 1 10 30 1 10 30
D
Realtive Gelatinolysis
250
200
150
100
50
0
CoMCont + - - - - - - -
CoMTb - + - - - + + +
IL-23 (ng/ml) - - 1 10 30 1 10 30

Figure S4

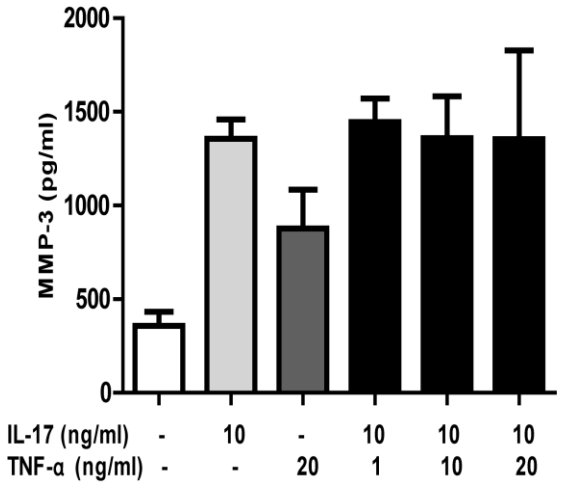
2000
1500
1000
500
0
MMP-3 (pg/ml)
IL-17 (ng/ml) - 10 - 10 10 10
TNF-α (ng/ml) - - 20 1 10 20

Figure S5

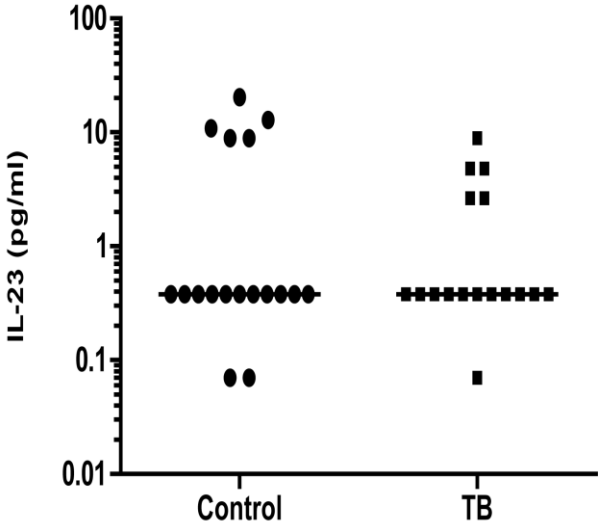

Figure S6

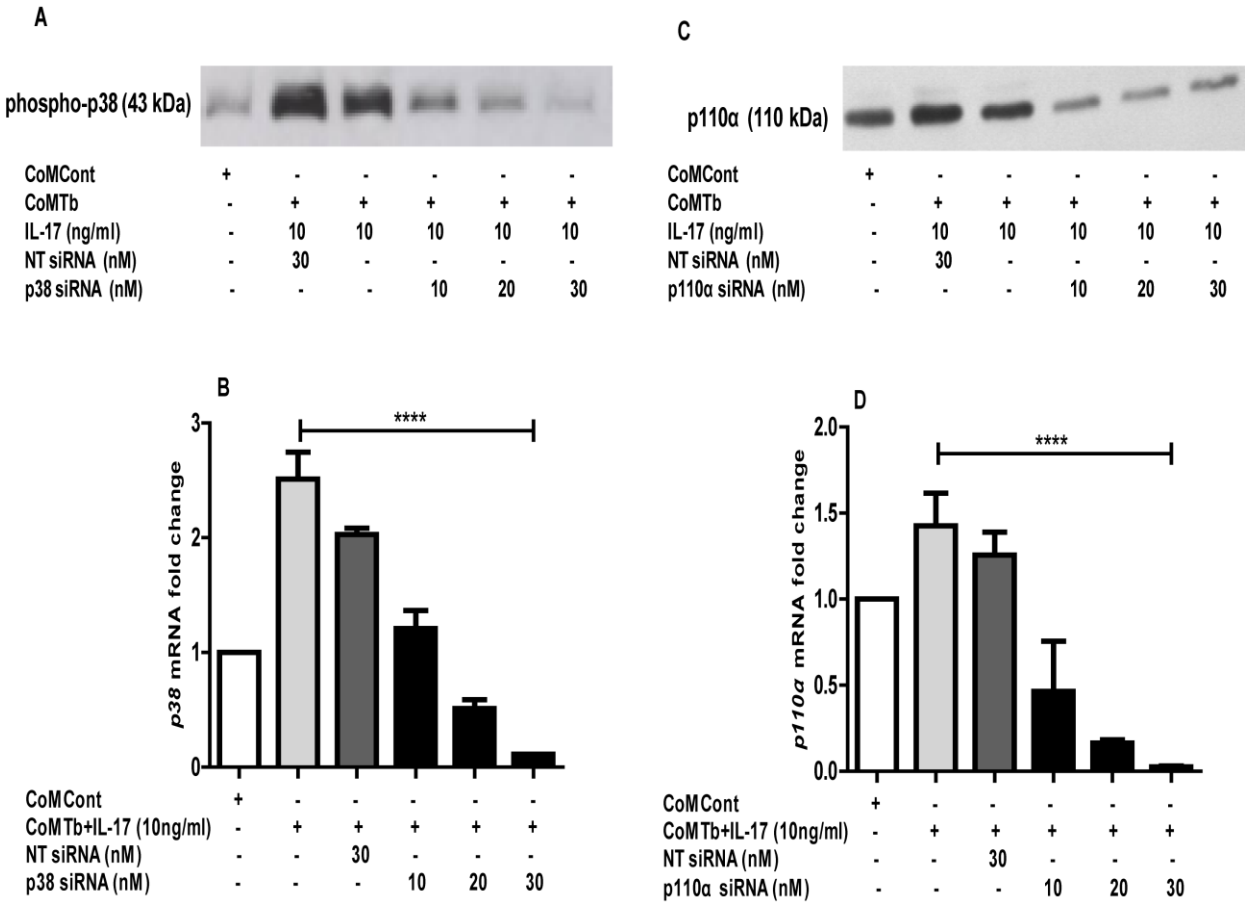
A
phospho-p38 (43 kDa)
CoMCont + - - - - -
CoMTb - + + + + +
IL-17 (ng/ml) - 10 10 10 10 10
NT siRNA (nM) - 30 - - - -
p38 siRNA (nM) - - - 10 20 30
C
p110α (110 kDa)
CoMCont + - - - - -
CoMTb - + + + + +
IL-17 (ng/ml) - 10 10 10 10 10
NT siRNA (nM) - 30 - - - -
p110α siRNA (nM) - - - 10 20 30
B
p38 mRNA fold change
****
CoMCont + - - - - -
CoMTb+IL-17 (10ng/ml) - + + + + +
NT siRNA (nM) - - 30 - - -
p38 siRNA (nM) - - - 10 20 30
D
p110α mRNA fold change
****
CoMCont + - - - - -
CoMTb+IL-17 (10ng/ml) - + + + + +
NT siRNA (nM) - - 30 - - -
p110α siRNA (nM) - - - 10 20 30

Figure S7

Cytokine/ Chemokine	Mean concentration (pg/ml) in NHBEs stimulated with CoMTb	Mean concentration (pg/ml) in NHBEs stimulated with CoMTb +IL-17	p value
TNF-α	611	752	ns
IL-1RA	1774	2251	ns
MIP-1α	5896	5951	ns
CXCL-8	178708	409251	<0.001

Table S1. Cytokine and chemokine concentrations in the culture medium of normal human bronchial epithelial cells stimulated with CoMTb or CoMTb+IL-17

CXCL-8 concentration was up-regulated when NHBE's were stimulated with CoMTb and IL-17, compared to CoMTb alone ($p<0.001$). TNF-α, IL-1RA and MIP-1α levels were similar in both groups.

Cytokine/ Chemokine	CoMCont		CoMTb		p value
	Mean (pg/ml)	SEM	Mean (pg/ml)	SEM	
GM-CSF	3	0	559.8	374	<0.0001
G-CSF	3	0	1178	446.2	<0.0001
IL1-β	131.8	44.5	26274	8815	<0.0001
IL-6	1	0	41992	14227	<0.0001
TNF-α	1	0	785	303	<0.0001
IFN-γ	Undetectable	N/A	Undetectable	N/A	N/A
IL-12	2	0	1591	1072	<0.0001
IL1-RA	505.5	171.7	7970	2032	0.0020
CXCL-8	27.75	8.9	94865	49375	<0.0001
MIP1-α	4	0	198693	94784	<0.0001
MCP-1	7.25	1.25	1426	642.4	<0.0001
MIG	47	22	147.3	48.2	ns
IL-17	Undetectable	N/A	Undetectable	N/A	N/A

Table S2. Cytokine and chemokine concentrations in the culture medium of monocytes stimulated with CoMCont or CoMTb

Monocytes infected with Mtb (CoMTb) secreted significantly more GM-CSF, G-CSF, IL1-β, IL-6, TNF-α, IL-12, IL1-RA and chemokines than uninfected monocytes (CoMCont). IL-17 was undetectable in CoMTb.